GWTC-1: First LIGO/Virgo Gravitational-Wave Transient Catalog

Agata Trovato & Michał Bejger (APC)

APC Colloquium, 8.2.19

Outline

- ⋆ Introduction
- ⋆ O1-O2 transient GW catalog (GWTC-1)
- ⋆ Data-mining the observed population sample
- ⋆ Conclusions

Gravitation: Newton vs Einstein

LIGO-Virgo global detector network

Very precise rulers: measuring distances between free-falling bodies with laser light.

LIGO-Virgo broadband sensitivity curves

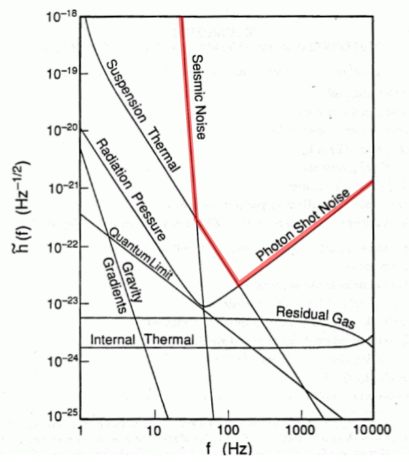

Initial LIGO proposal (1989)

- ⋆ Range of frequencies similar to human ears:

From 20 Hz (H0) to a few thousands Hz (3960 Hz, H7) - 8 octaves.

- ⋆ Poor, like for an ear, angular resolution.

Astrophysical sources: one-time events

Well-modelled signals (e.g. compact binary inspirals)

"Bursts" (signals difficult to model, e.g. supernovæ)

Astrophysical sources: persistent phenomena

”Continuous waves” (e.g. rotating non-axisymmetric neutron stars, wide binary systems)

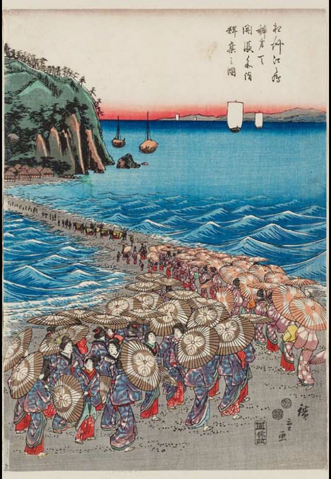

Stochastic background (populations of objects, waves from the early Universe)

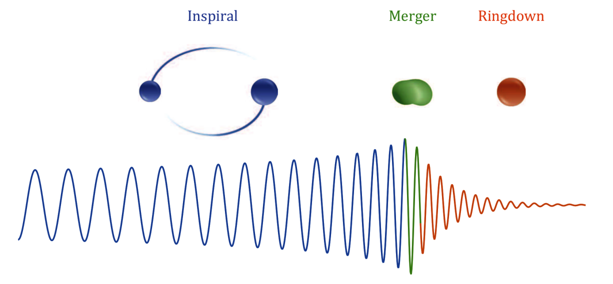

Inspiral
Merger
Ringdown

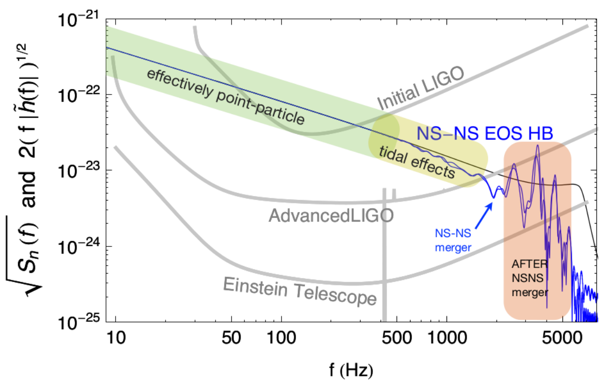

$\sqrt{S_n(f)}$ and $2(f\,|\tilde{h}(f)|)^{1/2}$
10^{-21}
10^{-22}
10^{-23}
10^{-24}
10^{-25}
effectively point-particle
Initial LIGO
NS–NS EOS HB
tidal effects
AdvancedLIGO
NS-NS
merger
AFTER
NSNS
merger
Einstein Telescope
10
50
100
500
1000
5000
f (Hz)

Gravitational waves intuitions

For a spherical wave of amplitude $h(r)$, flux of energy is $F(r) \propto h^2(r)$ and the luminosity $L(r) \propto 4\pi r^2 h^2(r)$.

Conservation of energy $\implies$ $h(r) \propto 1/r$

Consider a binary system of m_1 and m_2, semiaxis a with

- ⋆ total mass $M = m_1 + m_2$,
- ⋆ reduced mass $\mu = m_1 m_2 / M$,
- ⋆ mass quadrupole moment $Q \propto Ma^2$,
- ⋆ Kepler's third law $GM = a^3 \omega^2$.

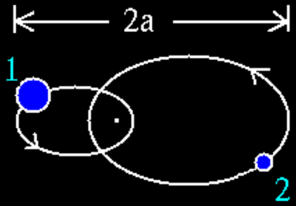

GWs correspond to accelerated movement of masses

$$h(r) \propto \frac{1}{r} \frac{\partial^2 (Ma^2)}{\partial t^2} \implies \boxed{\frac{G^2}{c^4} \frac{1}{r} \frac{M\mu}{a} = \frac{G^{5/3}}{c^4} \frac{1}{r} M^{2/3} \mu \, \omega^{2/3}.}$$

Binary system: chirp mass

Waves are emitted at the expense of the orbital energy:

$$E_{orb} = -\frac{Gm_1 m_2}{2a}, \qquad \frac{dE_{orb}}{dt} \equiv \frac{Gm_1 m_2}{2a^2}\dot{a} = -\frac{dE_{GW}}{dt}.$$

Resulting evolution of the orbital frequency ω:

$$\dot{\omega}^3 = \left(\frac{96}{5}\right)^3 \frac{\omega^{11}}{c^{15}} G^5 \mu^3 M^2 = \left(\frac{96}{5}\right)^3 \frac{\omega^{11}}{c^{15}} G^5 \mathcal{M}^5,$$

with chirp mass $\mathcal{M} = \left(\mu^3 M^2\right)^{1/5} = (m_1 m_2)^{3/5}/(m_1 + m_2)^{1/5}$.

Binary system GW frequency is primarily twice the orbital frequency ($2\pi f_{GW} = 2\omega$).

$\implies$ $\mathcal{M}$ is a directly measured quantity:

$$\mathcal{M} = \frac{c^3}{G}\left(\frac{5}{96}\pi^{-8/3} f_{GW}^{-11/3} \dot{f}_{GW}\right)^{3/5}.$$

Binary inspiral vs the sensitivity curve

Actually used in estimating the SNR is the frequency-domain match-filtering signal model $\tilde{h}(f)$ (Fourier transform of $h(t)$),

$$\tilde{h}(f) = Q(angles)\sqrt{\frac{5}{24}}\pi^{-2/3}\frac{\mathcal{M}^{5/6}}{r}f_{GW}^{-7/6}e^{-i\Psi(f)},$$

where the frequency domain phase Ψ is (in point-particle approximation):

$$\Psi(f) \equiv \Psi_{PP}(f) = 2\pi f t_c - \phi_c - \frac{\pi}{4} + \frac{3M}{128\mu v^{5/2}}\sum_{k=0}^{N}\alpha_k v^{k/2},$$

and v is a small parameter, e.g. the orbital velocity

$$v \propto (\pi M f_{GW})^{1/3}.$$

Binary system: source distance estimate

- ⋆ At cosmological distances, the observed frequency f_{GW} is redshifted by $(1 + z)$:

$$f \to f/(1 + z)$$

- ⋆ There is no mass scale in vacuum GR, so redshifting of f_{GW} cannot be distinguished from rescaling the masses

  because the signal's phase is expanded in powers of

$$v \propto (\pi M f_{GW})^{1/3}$$

$\Longrightarrow$ inferred masses are

$$m = (1 + z) m^{source}$$

$\Longrightarrow$ Direct, independent **luminosity distance** measurement (but not z) from GW with f_{GW} and the strain h:

$$r = \frac{5}{96\pi^2} \frac{c}{h} \frac{\dot{f}_{GW}}{f_{GW}^3}.$$

Binary system: distance-inclination degeneracy

Luminosity distance $\sim 1/h$.
In addition,

$$h = h_+ F_+ + h_\times F_\times$$

depends on the inclination of the binary with repect to the "line of sight".

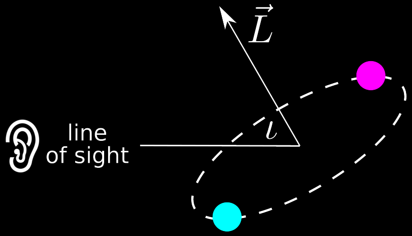

Two independent polarizations h_+ and $h_\times$:

$$h_+ = \frac{2\mu}{r} v^2 \left(1 + \cos^2 \iota\right) \cos\left(2\phi(t)\right),$$

$$h_\times = \frac{4\mu}{r} v^2 \cos \iota \sin\left(2\phi(t)\right)$$

Realistic binary: 15+ parameters

- Intrinsic:
  - masses
  - spins
  - tidal deformability

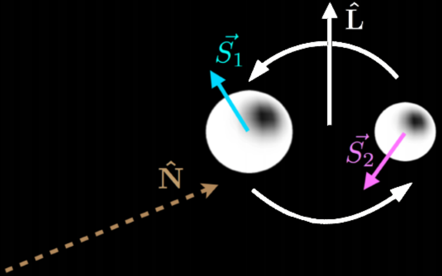

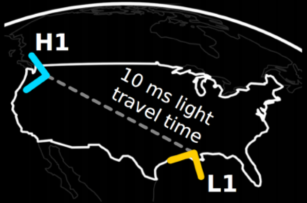

Credit: LIGO/Virgo

- Extrinsic:
  - Inclination, distance, polarisation
  - Sky location
  - Time, reference phase

GWTC-1

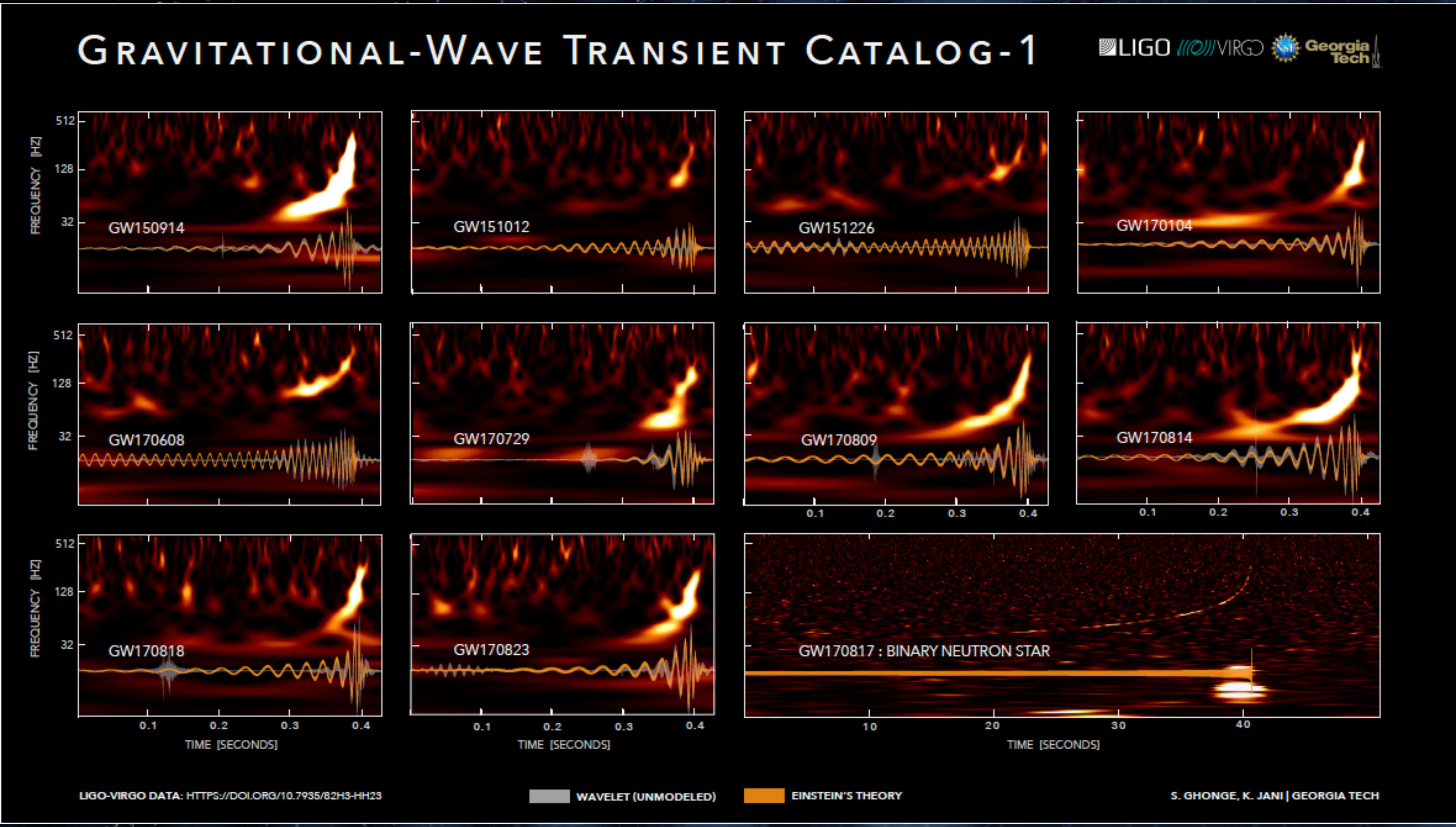

LVC, arXiv:1811.12907 [astro-ph]
submitted to PRX

Analysed data

- First Observing run **O1**:
  - ✓ 12/09/2015 -> 19/01/2016
  - ✓ Only LIGO detectors
  - ✓ Coincident analysis time HL: 48.6 days
- Second Observing run **O2**:
  - ✓ 30/11/2016 -> 25/08/2017 (LIGO)
  - ✓ Virgo since 1st August 2017
  - ✓ HL: 118 days
  - ✓ HLV: 15 days
- O1+O2: total HL coincident time = 166.6 days
- Upper plot: BNS range for each instrument during O2
- Lower plot: representative amplitude spectral density of the total strain noise

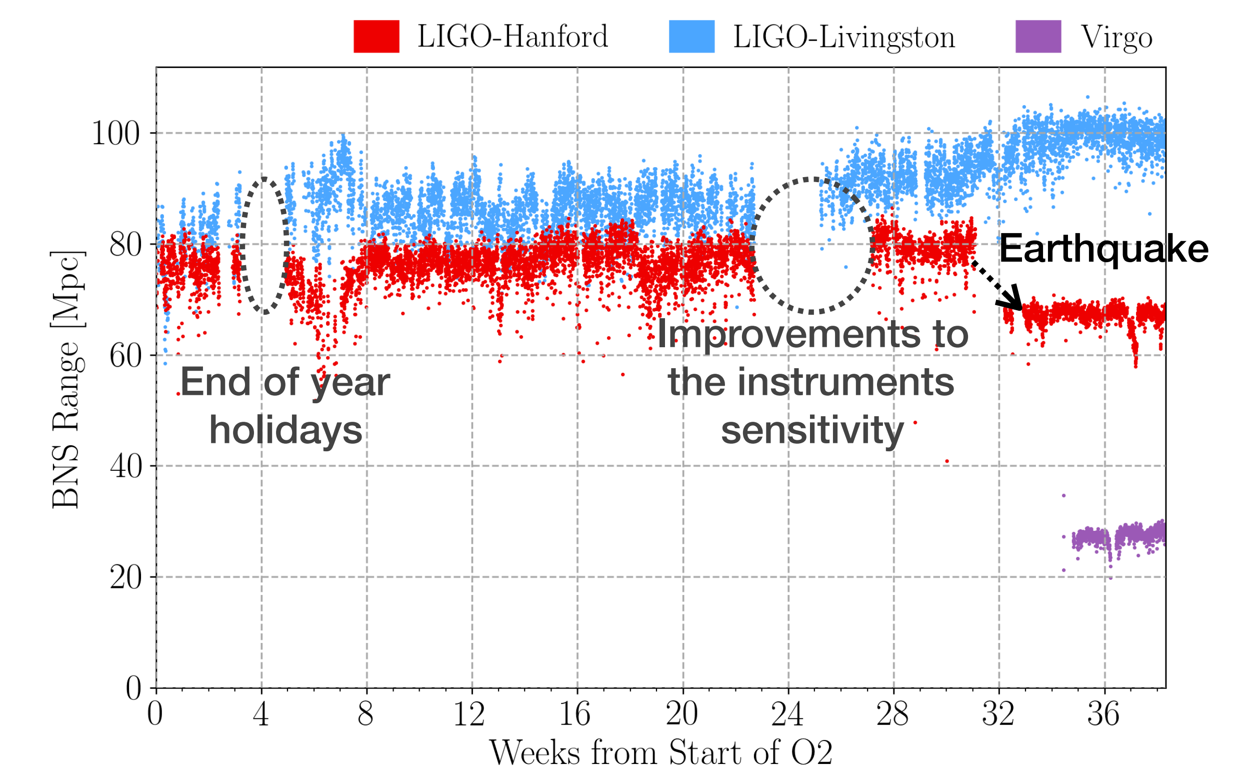

Best performance of each detector during O2

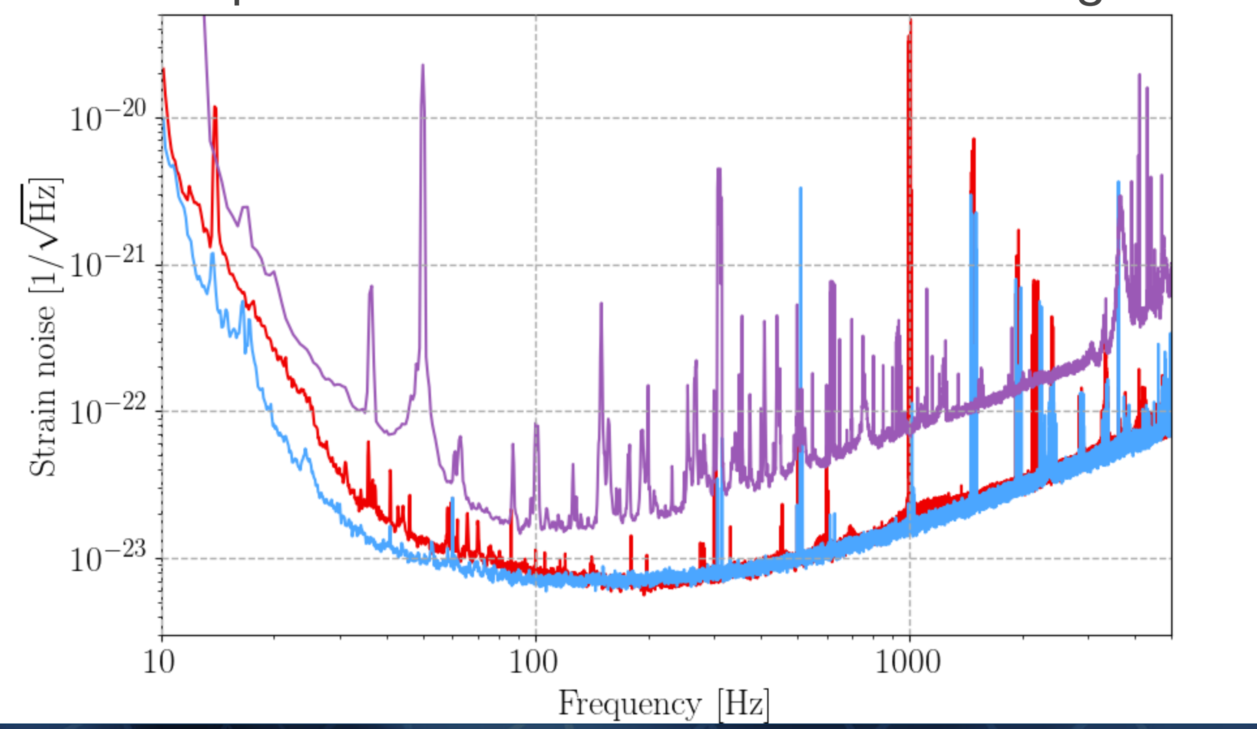

Search pipelines

- Given GWs emitted by a compact binary coalescence (**CBC**) in detector data compute:
  - ✓ CASE A: Cross-correlation (matched filter) between detector data and a bank of template waveforms predicted by general relativity
    - Total mass range: 2-500$M_\odot$ (**PyCBC**) and 2-400$M_\odot$ (**GstLAL**)
    - GstLAL includes Virgo data for the searches in August
  - ✓ CASE B: Coincident excess power in time-frequency representations of the detector strain data & assume that signals are "chirping" -> weakly modeled (or unmodeled)
    - Total mass range: <100$M_\odot$ for **cWB**
    - Network correlation coefficient (< 0.7) used to reject potential glitches
- Find coincident triggers from searches:
  - ✓ CASE A: Identify single detector triggers using tailored statistic that depends on SNR; look for temporal coincidence of triggers between detectors
  - ✓ CASE B: Find events that are coherent in multiple detectors.
- This analysis incorporates improvements in search pipelines since O1.

Search significance

- Assign statistical significance to coincident triggers:
  - ✓ **Ranking statistics:**
    - matched-filter searches: likelihood-ratio of obtaining the trigger parameters in the presence of a signal vs. in the presence of noise alone
    - Unmodeled searches: coherent network SNR
  - ✓ **Background estimate:**
    - time-shift triggers from one detector
    - resulting coincident triggers sample the background
  - ✓ **Inverse false-alarm-rate (IFAR):** quantifies the statistical significance of a trigger
    - **FAR** of foreground trigger = number of background triggers with equal or larger ranking divided by the duration of the data searched

Event selection

- Goal: Identify all events that are **confidently astrophysical** in origin, and additionally provide a manageable set of **marginal triggers** that may include some true signals, but certainly also includes noise triggers.
- **Threshold I: estimated FAR < 1 per 30 days (~12.2 per year)**
- **Threshold II: probability of astrophysical origin greater than 50%.**
- Events satisfying thresholds I & II: "GW" designation = confident detections. Note that the "LVC" nomenclature have been retired
- Events satisfying threshold I, but failing II designated as "marginal" (astrophysical origin cannot be established nor excluded unambiguosely)
- Thresholds to be satisfied in at least one of the two matched-filter searches.

Gravitational wave Events

- **11 confident detections**: 10 Binary Black Holes (BBH) + 1 Neutron Star (NS)
  - ✓ Already announced (7): GW150914, GW151012 (increased significance), GW151226, GW170104, GW170608, GW170814, GW170817
  - ✓ New ones (4): GW170729 (highest mass and further observed to date), GW170809, GW170818, GW170823
- **14 marginal triggers**
- *Note: events already announced… Why re-analysis?*
  - ✓ ***O1:*** *pipelines undergone improvements since O1 + expansion of the parameter space*
  - ✓ ***O2:*** *updates of the data itself due to data cleaning procedure*

Data release - GWOSC

https://www.gw-openscience.org/catalog/

Gravitational Wave Open Science Center

- Getting Started
- Data
  - Catalogs
  - Bulk Data
- Tutorials
- Software
- Detector Status
- Timelines
- My Sources
- GPS ↔ UTC
- About the detectors
- Projects
- Acknowledge GWOSC

Catalogs

GWTC-1

Gravitational-Wave Transient Catalog of Compact Binary Mergers (O1 & O2)

Documentation: Notes
Strain Data: Confident detections | Marginal Triggers
Auxillary Data: PE Samples, Skymaps, and more

Older event releases

Previous event releases are also available.

JSON Parameter Table — Show/hide columns

SORT: PRIMARY MASS (M_SUN) ↑

Event	Primary mass (M_sun)	Secondary mass (M_sun)	Effective inspiral spin	chirp mass (M_sun)	Final spin	Final mass (M_sun)	Luminosity distance (Mpc)	GPS time (s)
GW150914	$35.6^{+4.8}_{-3.0}$	$30.6^{+3.0}_{-4.4}$	$-0.01^{+0.12}_{-0.13}$	$28.6^{+1.6}_{-1.5}$	$0.69^{+0.05}_{-0.04}$	$63.1^{+3.3}_{-3.0}$	430^{+150}_{-170}	1126259462.4
GW151012	$23.3^{+14.0}_{-5.5}$	$13.6^{+4.1}_{-4.8}$	$0.04^{+0.28}_{-0.19}$	$15.2^{+2.0}_{-1.1}$	$0.67^{+0.13}_{-0.11}$	$35.7^{+9.9}_{-3.8}$	1060^{+540}_{-480}	1128678900.4
GW151226	$13.7^{+8.8}_{-3.2}$	$7.7^{+2.2}_{-2.6}$	$0.18^{+0.20}_{-0.12}$	$8.9^{+0.3}_{-0.3}$	$0.74^{+0.07}_{-0.05}$	$20.5^{+6.4}_{-1.5}$	440^{+180}_{-190}	1135136350.6
GW170104	$31.0^{+7.2}_{-5.6}$	$20.1^{+4.9}_{-4.5}$	$-0.04^{+0.17}_{-0.20}$	$21.5^{+2.1}_{-1.7}$	$0.66^{+0.08}_{-0.10}$	$49.1^{+5.2}_{-3.9}$	960^{+430}_{-410}	1167559936.6
GW170608	$10.9^{+5.3}_{-1.7}$	$7.6^{+1.3}_{-2.1}$	$0.03^{+0.19}_{-0.07}$	$7.9^{+0.2}_{-0.2}$	$0.69^{+0.04}_{-0.04}$	$17.8^{+3.2}_{-0.7}$	320^{+120}_{-110}	1180922494.5
GW170729	$50.6^{+16.6}_{-10.2}$	$34.3^{+9.1}_{-10.1}$	$0.36^{+0.21}_{-0.25}$	$35.7^{+6.5}_{-4.7}$	$0.81^{+0.07}_{-0.13}$	$80.3^{+14.6}_{-10.2}$	2750^{+1350}_{-1320}	1185389807.3
GW170809	$35.2^{+8.3}_{-6.0}$	$23.8^{+5.2}_{-5.1}$	$0.07^{+0.16}_{-0.16}$	$25.0^{+2.1}_{-1.6}$	$0.70^{+0.08}_{-0.09}$	$56.4^{+5.2}_{-3.7}$	990^{+320}_{-380}	1186302519.8
GW170814	$30.7^{+5.7}_{-3.0}$	$25.3^{+2.9}_{-4.1}$	$0.07^{+0.12}_{-0.11}$	$24.2^{+1.4}_{-1.1}$	$0.72^{+0.07}_{-0.05}$	$53.4^{+3.2}_{-2.4}$	580^{+160}_{-210}	1186741861.5
GW170817	$1.46^{+0.12}_{-0.10}$	$1.27^{+0.09}_{-0.09}$	$0.00^{+0.02}_{-0.01}$	$1.186^{+0.001}_{-0.001}$	≤ 0.89	≤ 2.8	40^{+10}_{-10}	1187008882.4
GW170818	$35.5^{+7.5}_{-4.7}$	$26.8^{+4.3}_{-5.2}$	$-0.09^{+0.18}_{-0.21}$	$26.7^{+2.1}_{-1.7}$	$0.67^{+0.07}_{-0.08}$	$59.8^{+4.8}_{-3.8}$	1020^{+430}_{-360}	1187058327.1
GW170823	$39.6^{+10.0}_{-6.6}$	$29.4^{+6.3}_{-7.1}$	$0.08^{+0.20}_{-0.22}$	$29.3^{+4.2}_{-3.2}$	$0.71^{+0.08}_{-0.10}$	$65.6^{+9.4}_{-6.6}$	1850^{+840}_{-840}	1187529256.5

GWTC-1-confident

GW170814

Effective inspiral spin,	$0.07^{+0.12}_{-0.11}$
Luminosity distance, *Mpc*	580^{+160}_{-210}
Final spin,	$0.72^{+0.07}_{-0.05}$
Primary mass, *M_sun*	$30.7^{+5.7}_{-3.0}$
FAR gstLAL, *yr^-1*	< 1.00e-07
FAR PyCBC, *yr^-1*	< 1.25e-05
Secondary mass, *M_sun*	$25.3^{+2.9}_{-4.1}$
chirp mass, *M_sun*	$24.2^{+1.4}_{-1.1}$
Radiated energy, *M_sun X c^2*	$2.7^{+0.4}_{-0.3}$
Network SNR gstLAL,	15.9
Source redshift,	$0.12^{+0.03}_{-0.04}$
FAR cWB, *yr^-1*	< 2.08e-04
UTCtime,	10:30:43.5
Peak luminosity, *10^56 erg s^-1*	$3.7^{+0.4}_{-0.5}$
Sky localization, *deg^2*	87
Final mass, *M_sun*	$53.4^{+3.2}_{-2.4}$
GPS time (s),	1186741861.5
Network SNR PyCBC,	16.3
Network SNR cWB,	17.2

Download Data Files:

V1 4096sec 4KHz	V-V1_GWOSC_4KHZ_R1-1186739814-4096.hdf5 V-V1_GWOSC_4KHZ_R1-1186739814-4096.gwf V-V1_GWOSC_4KHZ_R1-1186739814-4096.txt.gz
V1 4096sec 16KHz	V-V1_GWOSC_16KHZ_R1-1186739814-4096.hdf5 V-V1_GWOSC_16KHZ_R1-1186739814-4096.gwf V-V1_GWOSC_16KHZ_R1-1186739814-4096.txt.gz
V1 32sec 4KHz	V-V1_GWOSC_4KHZ_R1-1186741846-32.hdf5 V-V1_GWOSC_4KHZ_R1-1186741846-32.gwf V-V1_GWOSC_4KHZ_R1-1186741846-32.txt.gz
V1 32sec 16KHz	V-V1_GWOSC_16KHZ_R1-1186741846-32.hdf5 V-V1_GWOSC_16KHZ_R1-1186741846-32.gwf V-V1_GWOSC_16KHZ_R1-1186741846-32.txt.gz

- h(t) strain data, PE samples, skymap FITS files, …
- Full O2 strain data: end of Feb 2019

Observed events vs IFAR

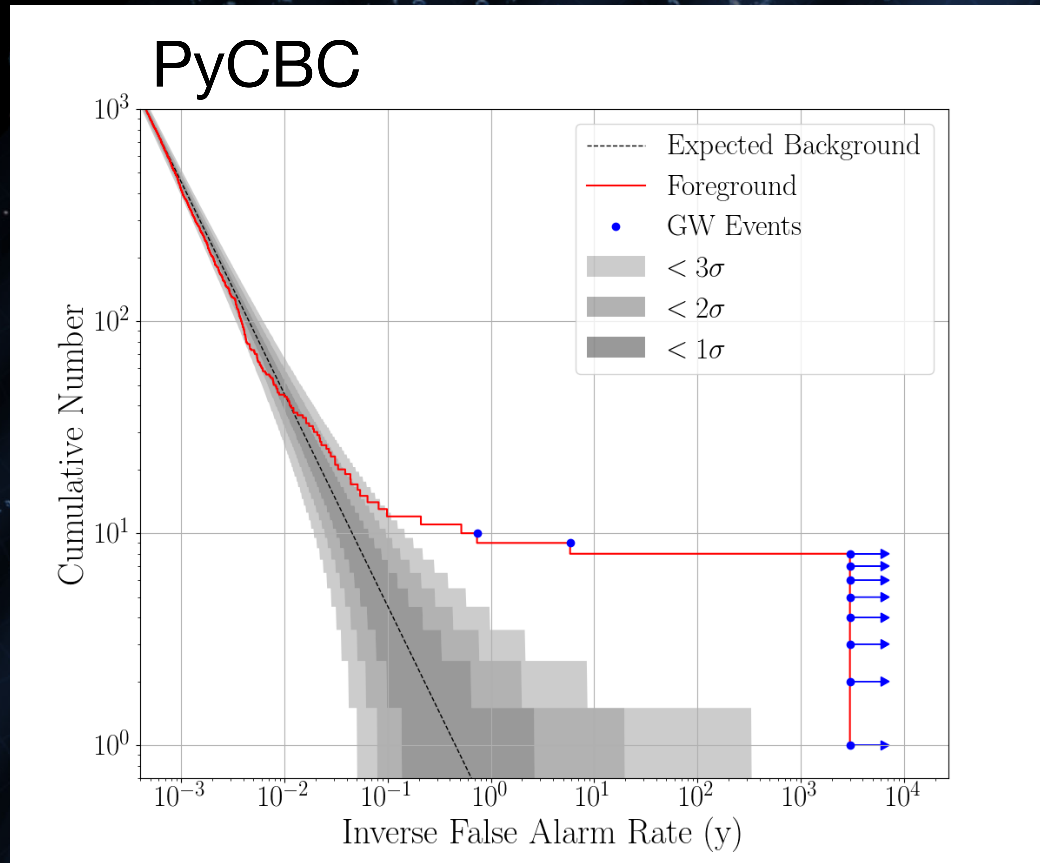

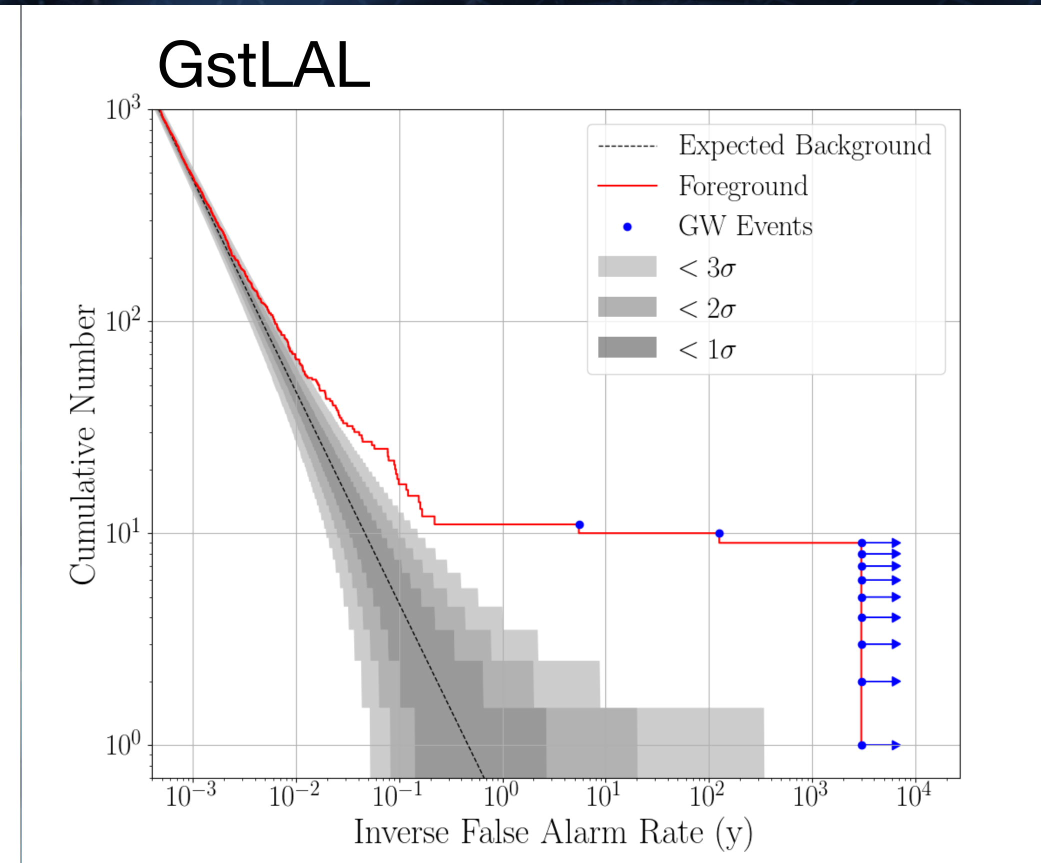

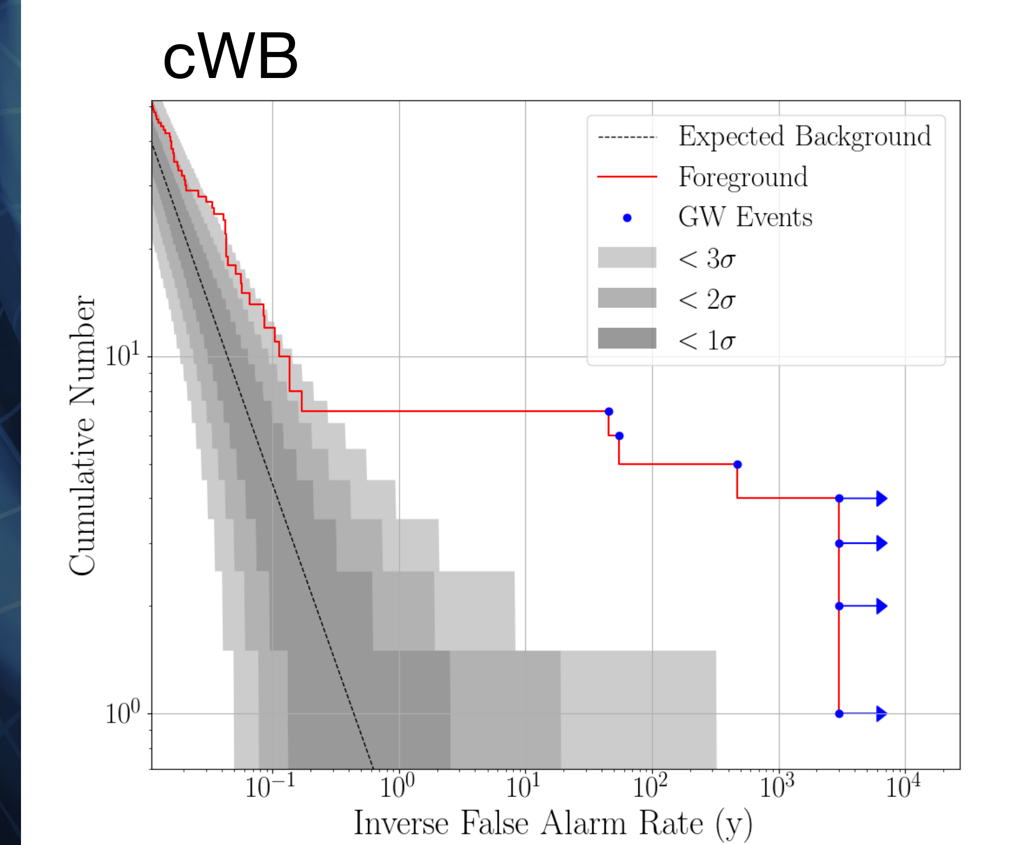

- Observed distribution of events against IFAR.
- Expected background for the analysis time with Poisson uncertainty bands.
- The foreground **events** (blue dots, $p_{astro} > 0.5$) clearly stand out from the background.
- Arrows used for events with IFAR> 3000 y
- Not all events were found by all pipelines

Confident GW detections

Event	UTC Time	FAR [y^{-1}] PyCBC	FAR [y^{-1}] GstLAL	FAR [y^{-1}] cWB	Network SNR PyCBC	Network SNR GstLAL	Network SNR cWB
GW150914	09:50:45.4	$< 1.53 \times 10^{-5}$	$< 1.00 \times 10^{-7}$	$< 1.63 \times 10^{-4}$	23.6	24.4	25.2
GW151012	09:54:43.4	0.17	7.92×10^{-3}	–	9.5	10.0	–
GW151226	03:38:53.6	$< 1.69 \times 10^{-5}$	$< 1.00 \times 10^{-7}$	0.02	13.1	13.1	11.9
GW170104	10:11:58.6	$< 1.37 \times 10^{-5}$	$< 1.00 \times 10^{-7}$	2.91×10^{-4}	13.0	13.0	13.0
GW170608	02:01:16.5	$< 3.09 \times 10^{-4}$	$< 1.00 \times 10^{-7}$	1.44×10^{-4}	15.4	14.9	14.1
GW170729	18:56:29.3	1.36	0.18	0.02	9.8	10.8	10.2
GW170809	08:28:21.8	1.45×10^{-4}	$< 1.00 \times 10^{-7}$	–	12.2	12.4	–
GW170814	10:30:43.5	$< 1.25 \times 10^{-5}$	$< 1.00 \times 10^{-7}$	$< 2.08 \times 10^{-4}$	16.3	15.9	17.2
GW170817	12:41:04.4	$< 1.25 \times 10^{-5}$	$< 1.00 \times 10^{-7}$	–	30.9	33.0	–
GW170818	02:25:09.1	–	4.20×10^{-5}	–	–	11.3	–
GW170823	13:13:58.5	$< 3.29 \times 10^{-5}$	$< 1.00 \times 10^{-7}$	2.14×10^{-3}	11.1	11.5	10.8

- Four new binary black holes: GW170729, GW170809 (also on-line), GW170818, GW170823 (also on-line)
- 151012 designated as a GW event, previously denoted as LVT (higher significance because of improved detection pipelines)
- Not all events found with all searches
- GW170817 remains the event with the highest network SNR

The "Sirens of August"

- ⋆ 5 GW events in August 2017 (10% of the total observing time)
- ⋆ 10 non-overlapping periods of similar duration, with an average GW event rate of 1.1 per period.
- ⋆ Assuming a Poisson process, the probability of 5 events or more in at least one such periods is 5.3%.

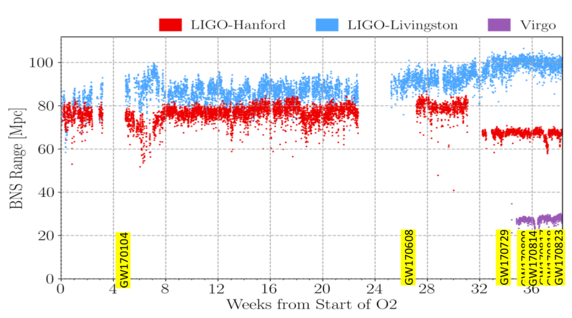

$\Longrightarrow$ Seeing 5 events in one month is statistically consistent with our expectations from Poissonian statistics (see `dcc.ligo.org/LIGO-T1800529/public` for details)

Marginal triggers

- FAR < 1 per 30 days but $p_{astro}<0.5$
- Some of these marginal triggers may be of astrophysical origin; we cannot determine which.
- 9 triggers have excess power from known source of noise
  - 4 of these: instrumental artifact overlaps the signal region, and may account for the strain amplitude of the marginal trigger.

Date	UTC	Search	FAR [y^{-1}]	Network SNR	$\mathcal{M}^{det}$ [$M_\odot$]	Data Quality
151008	14:09:17.5	PyCBC	10.17	8.8	5.12	No artifacts
151012A	06:30:45.2	GstLAL	8.56	9.6	2.01	Artifacts present
151116	22:41:48.7	PyCBC	4.77	9.0	1.24	No artifacts
161202	03:53:44.9	GstLAL	6.00	10.5	1.54	Artifacts can account for
161217	07:16:24.4	GstLAL	10.12	10.7	7.86	Artifacts can account for
170208	10:39:25.8	GstLAL	11.18	10.0	7.39	Artifacts present
170219	14:04:09.0	GstLAL	6.26	9.6	1.53	No artifacts
170405	11:04:52.7	GstLAL	4.55	9.3	1.44	Artifacts present
170412	15:56:39.0	GstLAL	8.22	9.7	4.36	Artifacts can account for
170423	12:10:45.0	GstLAL	6.47	8.9	1.17	No artifacts
170616	19:47:20.8	PyCBC	1.94	9.1	2.75	Artifacts present
170630	16:17:07.8	GstLAL	10.46	9.7	0.90	Artifacts present
170705	08:45:16.3	GstLAL	10.97	9.3	3.40	No artifacts
170720	22:44:31.8	GstLAL	10.75	13.0	5.96	Artifacts can account for

Instrumental artifact

Scattered light

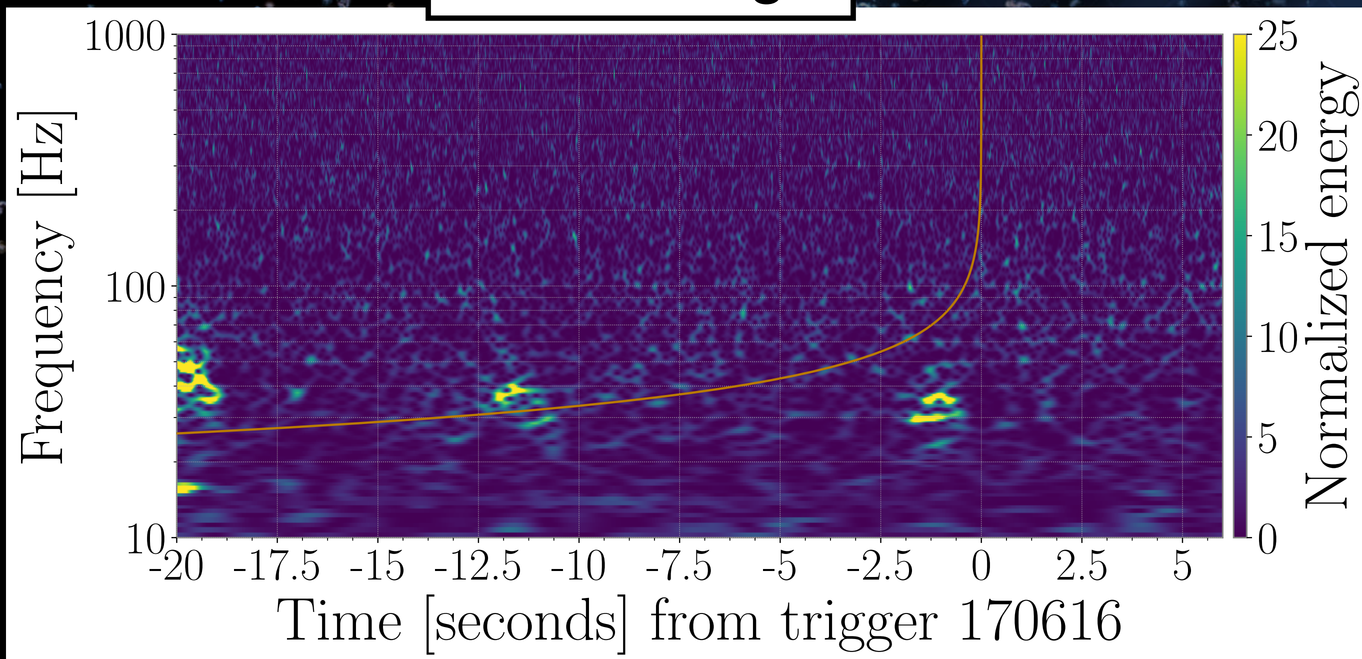

60-200 Hz non stationarity

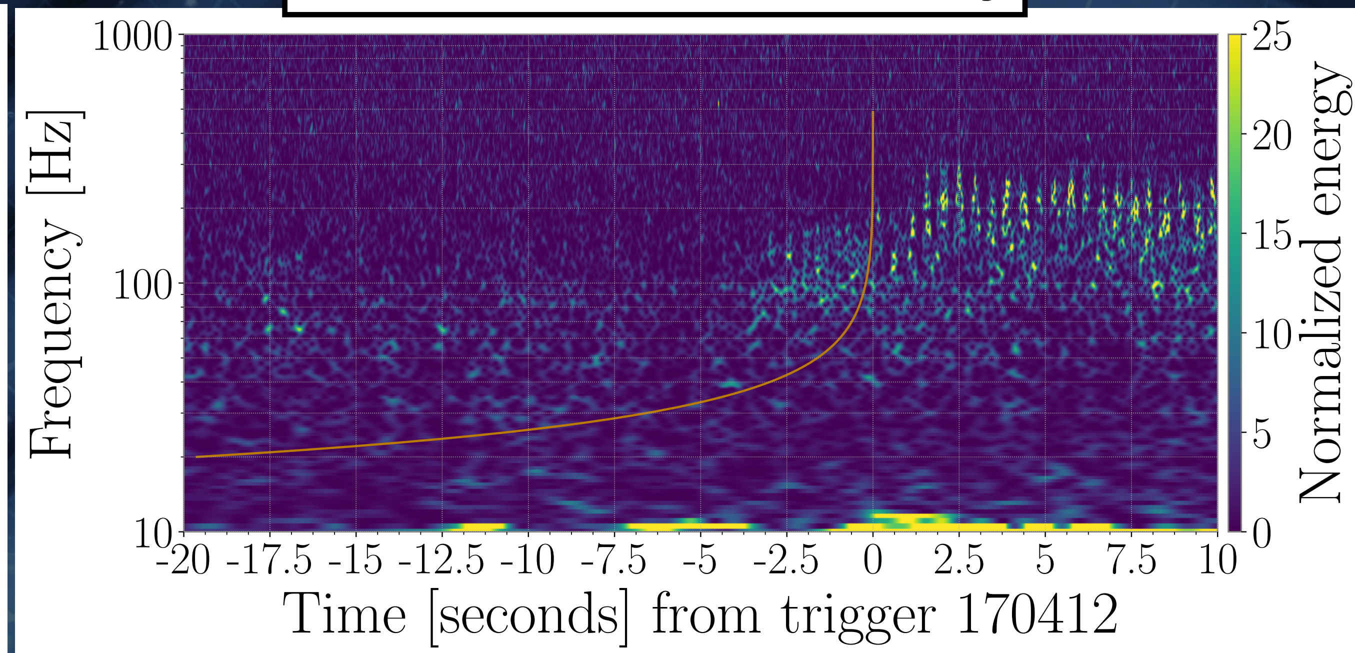

Short duration transient

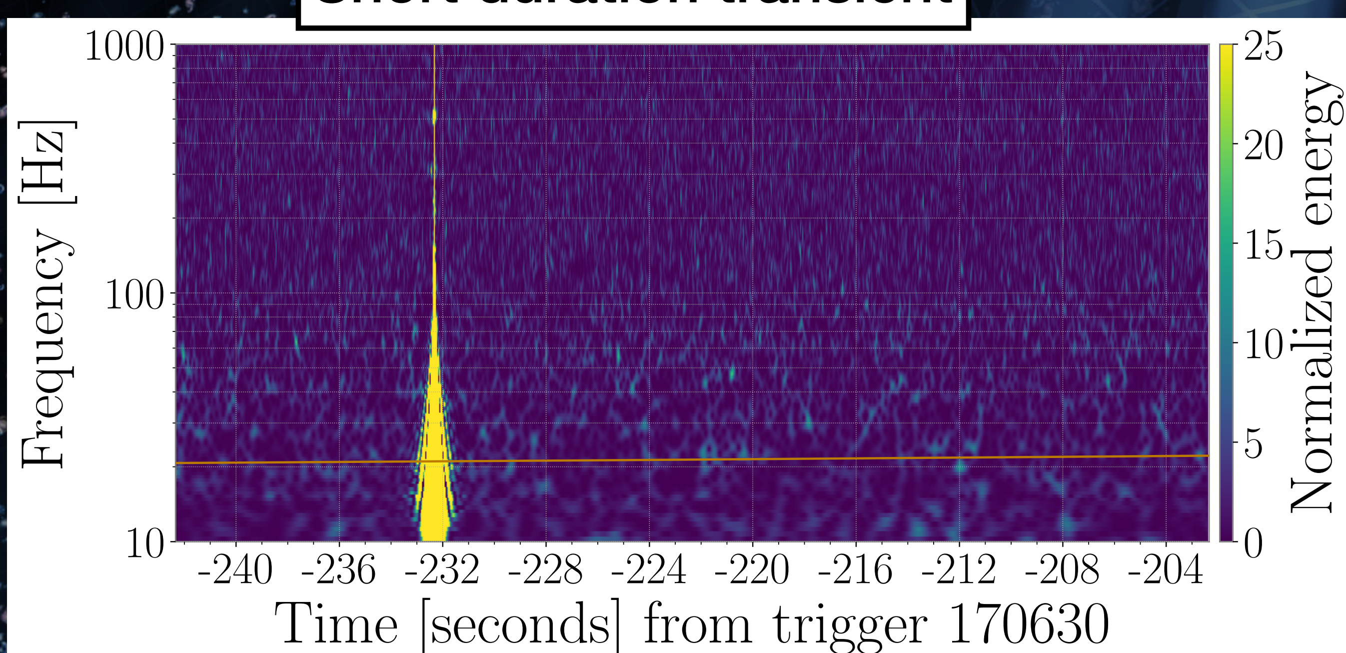

Blip

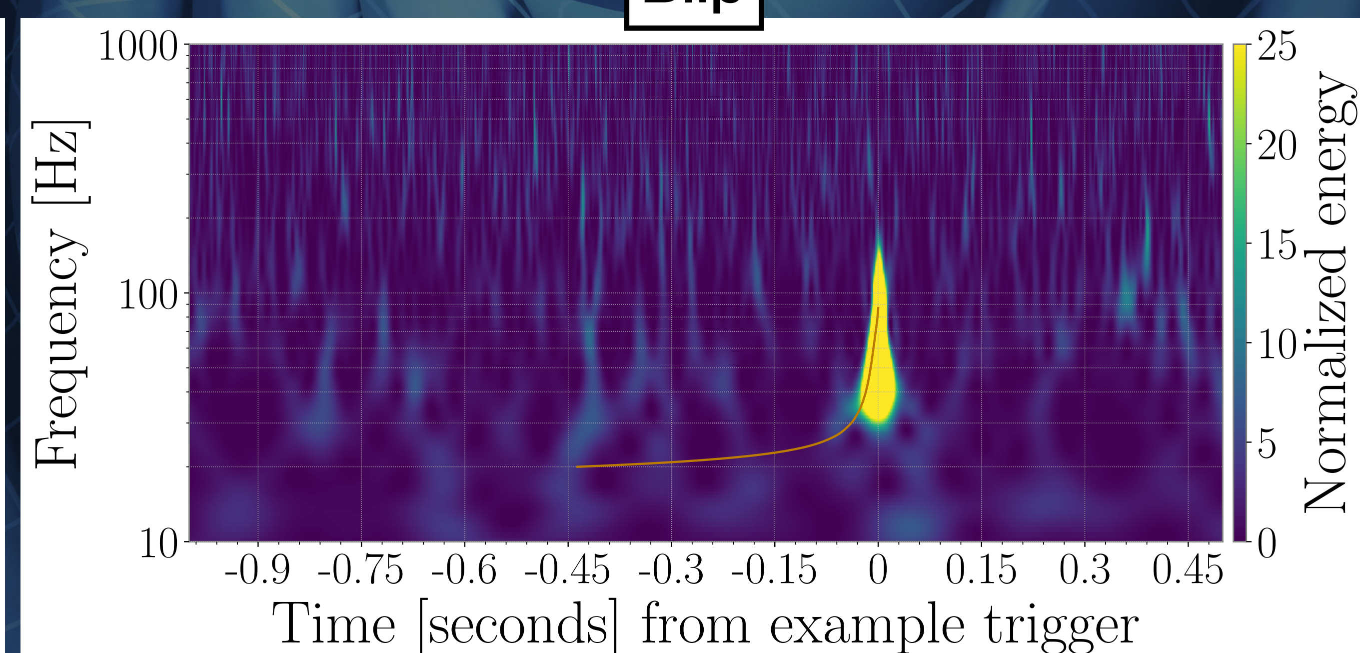

Parameter estimation

- Median values and 90% credible intervals based on two GR waveform models
- GW170729: highest mass and most distant BBH observed to date (median values); has moderate spin
- GW170818: best localised BBH to date - HLV detection
- Results consistent with previously published ones

Event	$m_1/\mathrm{M}_\odot$	$m_2/\mathrm{M}_\odot$	$\mathcal{M}/\mathrm{M}_\odot$	χ_{eff}	$M_{\mathrm{f}}/\mathrm{M}_\odot$	a_{f}	$E_{\mathrm{rad}}/(\mathrm{M}_\odot c^2)$	$\ell_{\mathrm{peak}}/(\mathrm{erg\,s^{-1}})$	d_L/Mpc	z	$\Delta\Omega/\mathrm{deg}^2$
GW150914	$35.6^{+4.8}_{-3.0}$	$30.6^{+3.0}_{-4.4}$	$28.6^{+1.6}_{-1.5}$	$-0.01^{+0.12}_{-0.13}$	$63.1^{+3.3}_{-3.0}$	$0.69^{+0.05}_{-0.04}$	$3.1^{+0.4}_{-0.4}$	$3.6^{+0.4}_{-0.4}\times 10^{56}$	430^{+150}_{-170}	$0.09^{+0.03}_{-0.03}$	179
GW151012	$23.3^{+14.0}_{-5.5}$	$13.6^{+4.1}_{-4.8}$	$15.2^{+2.0}_{-1.1}$	$0.04^{+0.28}_{-0.19}$	$35.7^{+9.9}_{-3.8}$	$0.67^{+0.13}_{-0.11}$	$1.5^{+0.5}_{-0.5}$	$3.2^{+0.8}_{-1.7}\times 10^{56}$	1060^{+540}_{-480}	$0.21^{+0.09}_{-0.09}$	1555
GW151226	$13.7^{+8.8}_{-3.2}$	$7.7^{+2.2}_{-2.6}$	$8.9^{+0.3}_{-0.3}$	$0.18^{+0.20}_{-0.12}$	$20.5^{+6.4}_{-1.5}$	$0.74^{+0.07}_{-0.05}$	$1.0^{+0.1}_{-0.2}$	$3.4^{+0.7}_{-1.7}\times 10^{56}$	440^{+180}_{-190}	$0.09^{+0.04}_{-0.04}$	1033
GW170104	$31.0^{+7.2}_{-5.6}$	$20.1^{+4.9}_{-4.5}$	$21.5^{+2.1}_{-1.7}$	$-0.04^{+0.17}_{-0.20}$	$49.1^{+5.2}_{-3.9}$	$0.66^{+0.08}_{-0.10}$	$2.2^{+0.5}_{-0.5}$	$3.3^{+0.6}_{-0.9}\times 10^{56}$	960^{+430}_{-410}	$0.19^{+0.07}_{-0.08}$	924
GW170608	$10.9^{+5.3}_{-1.7}$	$7.6^{+1.3}_{-2.1}$	$7.9^{+0.2}_{-0.2}$	$0.03^{+0.19}_{-0.07}$	$17.8^{+3.2}_{-0.7}$	$0.69^{+0.04}_{-0.04}$	$0.9^{+0.0}_{-0.1}$	$3.5^{+0.4}_{-1.3}\times 10^{56}$	320^{+120}_{-110}	$0.07^{+0.02}_{-0.02}$	396
GW170729	$50.6^{+16.6}_{-10.2}$	$34.3^{+9.1}_{-10.1}$	$35.7^{+6.5}_{-4.7}$	$0.36^{+0.21}_{-0.25}$	$80.3^{+14.6}_{-10.2}$	$0.81^{+0.07}_{-0.13}$	$4.8^{+1.7}_{-1.7}$	$4.2^{+0.9}_{-1.5}\times 10^{56}$	2750^{+1350}_{-1320}	$0.48^{+0.19}_{-0.20}$	1033
GW170809	$35.2^{+8.3}_{-6.0}$	$23.8^{+5.2}_{-5.1}$	$25.0^{+2.1}_{-1.6}$	$0.07^{+0.16}_{-0.16}$	$56.4^{+5.2}_{-3.7}$	$0.70^{+0.08}_{-0.09}$	$2.7^{+0.6}_{-0.6}$	$3.5^{+0.6}_{-0.9}\times 10^{56}$	990^{+320}_{-380}	$0.20^{+0.05}_{-0.07}$	340
GW170814	$30.7^{+5.7}_{-3.0}$	$25.3^{+2.9}_{-4.1}$	$24.2^{+1.4}_{-1.1}$	$0.07^{+0.12}_{-0.11}$	$53.4^{+3.2}_{-2.4}$	$0.72^{+0.07}_{-0.05}$	$2.7^{+0.4}_{-0.3}$	$3.7^{+0.4}_{-0.5}\times 10^{56}$	580^{+160}_{-210}	$0.12^{+0.03}_{-0.04}$	87
GW170817	$1.46^{+0.12}_{-0.10}$	$1.27^{+0.09}_{-0.09}$	$1.186^{+0.001}_{-0.001}$	$0.00^{+0.02}_{-0.01}$	≤ 2.8	≤ 0.89	≥ 0.04	$\geq 0.1\times 10^{56}$	40^{+10}_{-10}	$0.01^{+0.00}_{-0.00}$	16
GW170818	$35.5^{+7.5}_{-4.7}$	$26.8^{+4.3}_{-5.2}$	$26.7^{+2.1}_{-1.7}$	$-0.09^{+0.18}_{-0.21}$	$59.8^{+4.8}_{-3.8}$	$0.67^{+0.07}_{-0.08}$	$2.7^{+0.5}_{-0.5}$	$3.4^{+0.5}_{-0.7}\times 10^{56}$	1020^{+430}_{-360}	$0.20^{+0.07}_{-0.07}$	39
GW170823	$39.6^{+10.0}_{-6.6}$	$29.4^{+6.3}_{-7.1}$	$29.3^{+4.2}_{-3.2}$	$0.08^{+0.20}_{-0.22}$	$65.6^{+9.4}_{-6.6}$	$0.71^{+0.08}_{-0.10}$	$3.3^{+0.9}_{-0.8}$	$3.6^{+0.6}_{-0.9}\times 10^{56}$	1850^{+840}_{-840}	$0.34^{+0.13}_{-0.14}$	1651

Component masses

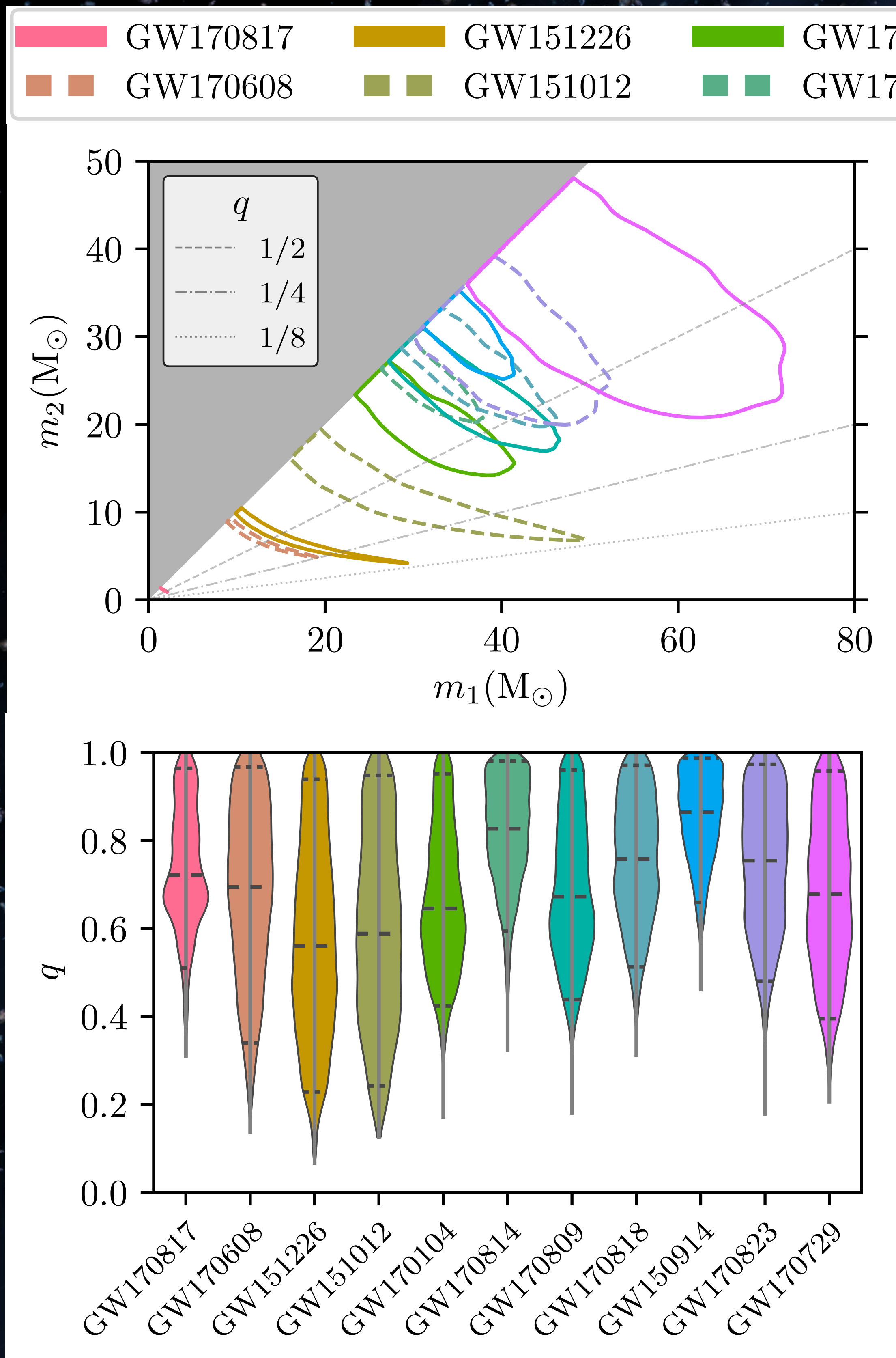

- **$m_1 \geq m_2$** —> shaded region excluded
- Component masses from ~5 $M_\odot$ to ~70 $M_\odot$
- BBH component masses show strong degeneracy with each other

- **$q = m_2/m_1 \leq 1$**
- Width of posteriors for q depends on the SNR (GW170817, GW150914, GW170814 best measured)
- GW151226 and GW151012 have posterior support for more unequal mass ratios

Spins

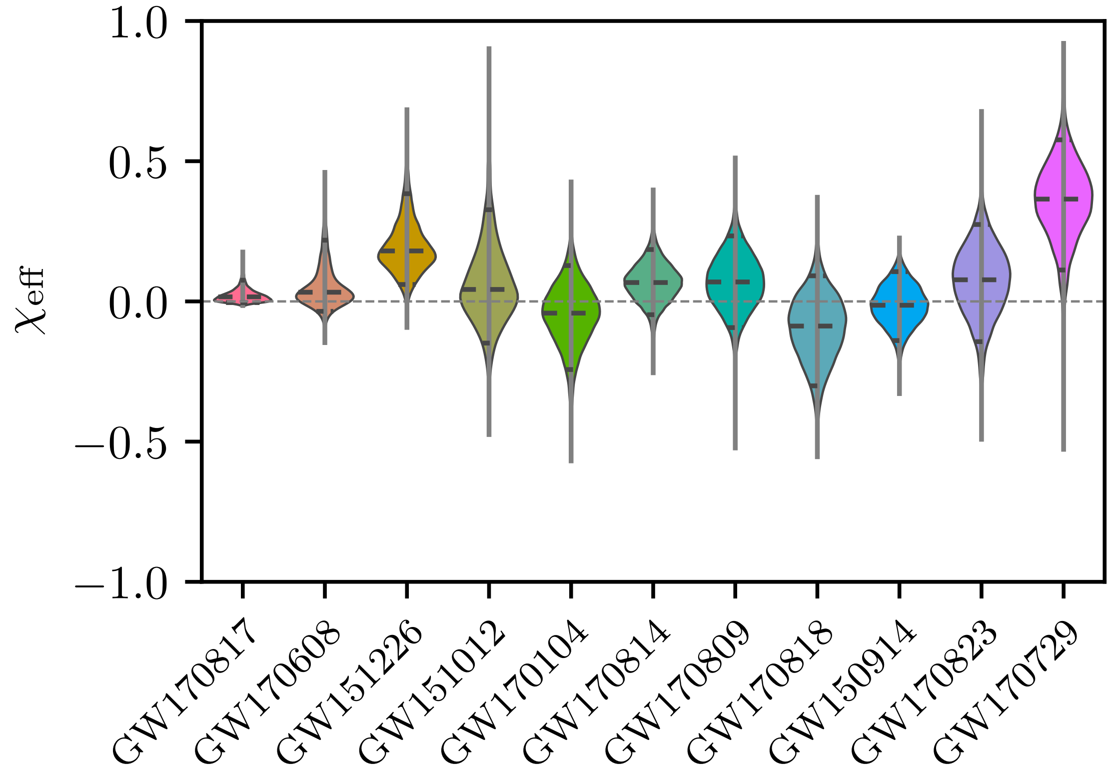

Effective aligned spin

$$\chi_{\mathrm{eff}} = \frac{m_1\chi_1 + m_2\chi_2}{m_1 + m_2}$$

$$\chi_i = \vec{S}_i \cdot \hat{L}/m_i^2$$

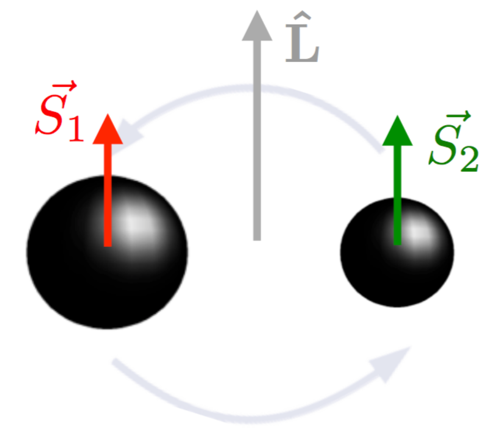

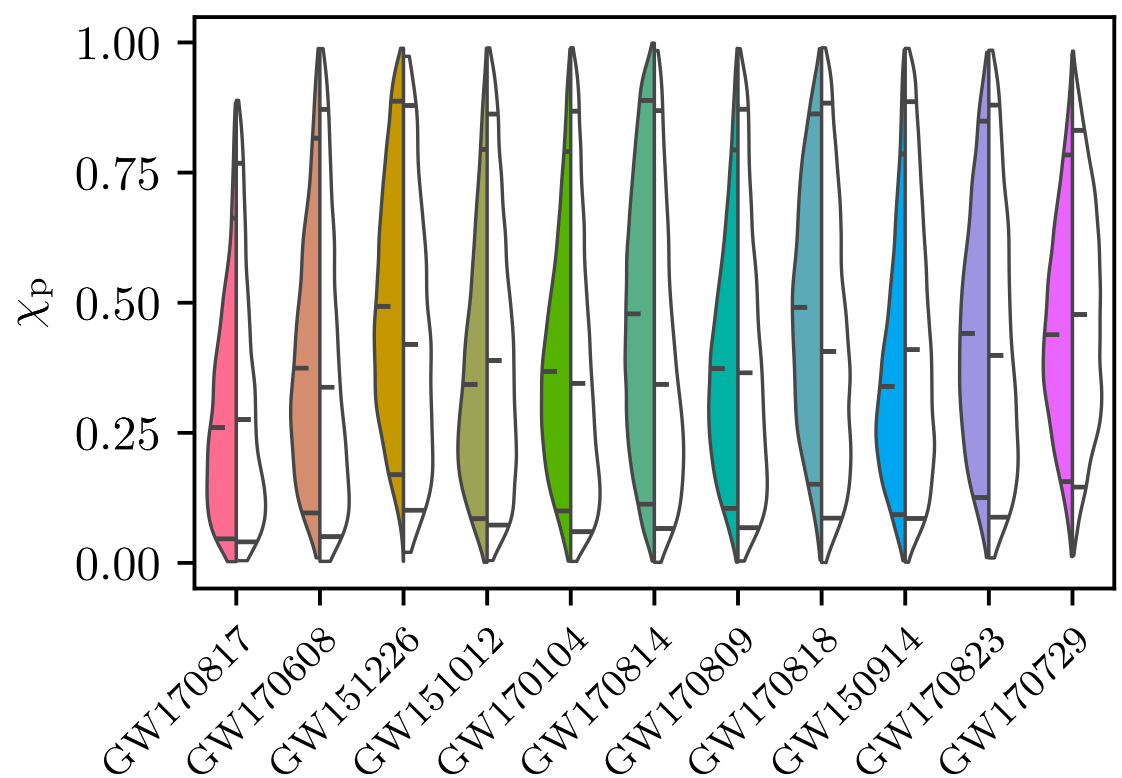

Effective precession spin

$$\chi_p = \frac{\max\left(A_1 m_1^2 \chi_{1\perp}, A_2 m_2^2 \chi_{2\perp}\right)}{A_1 m_1^2}$$

$$A_1 = 2 + 3m_2/2m_1,\ A_2 = 2 + 3m_1/2m_2$$

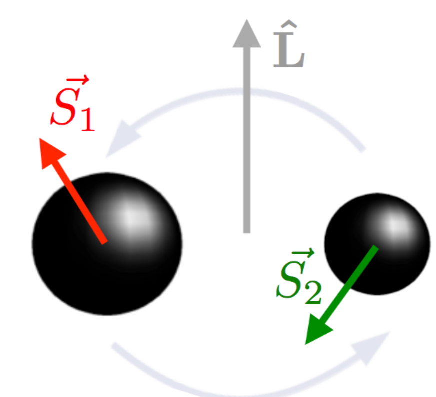

Spins

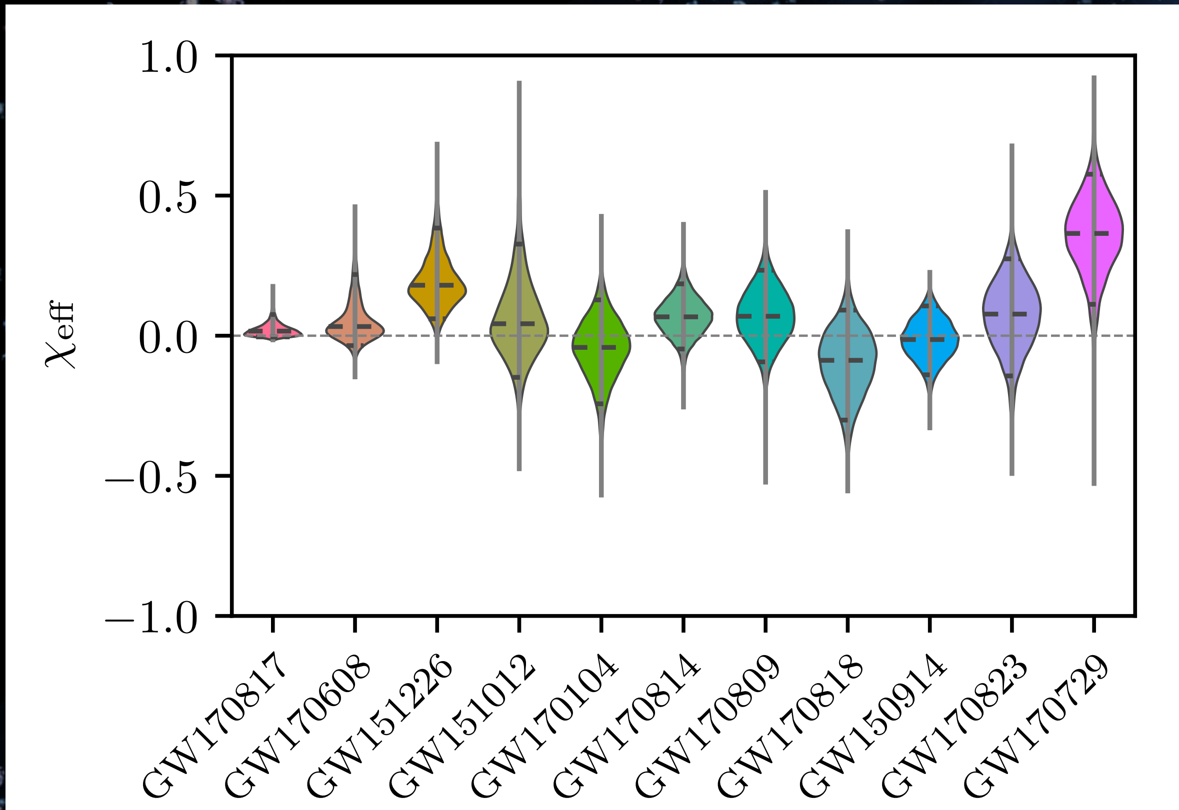

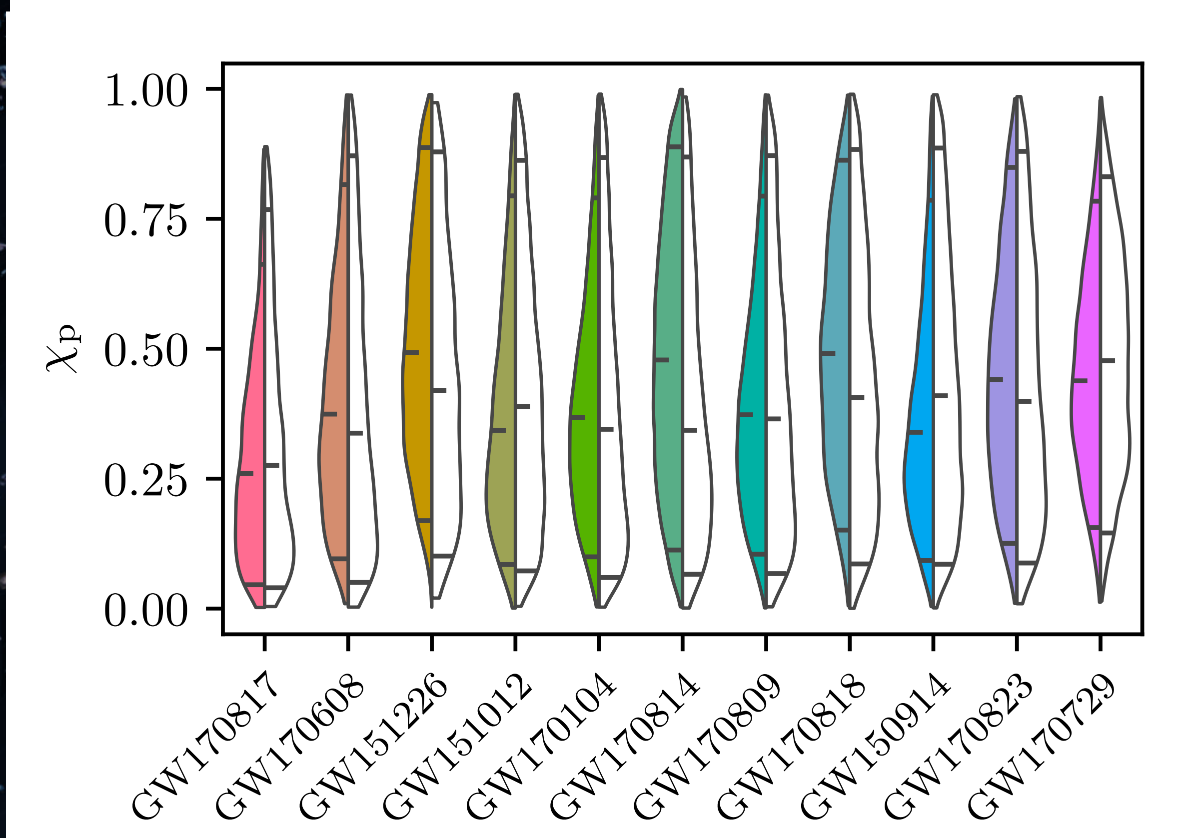

- Posteriors for aligned spin mostly peak around zero
- GW170729 has clear indication for a net positive spin

- Precession remains unconstrained for all events

Distance, inclination, chirp mass

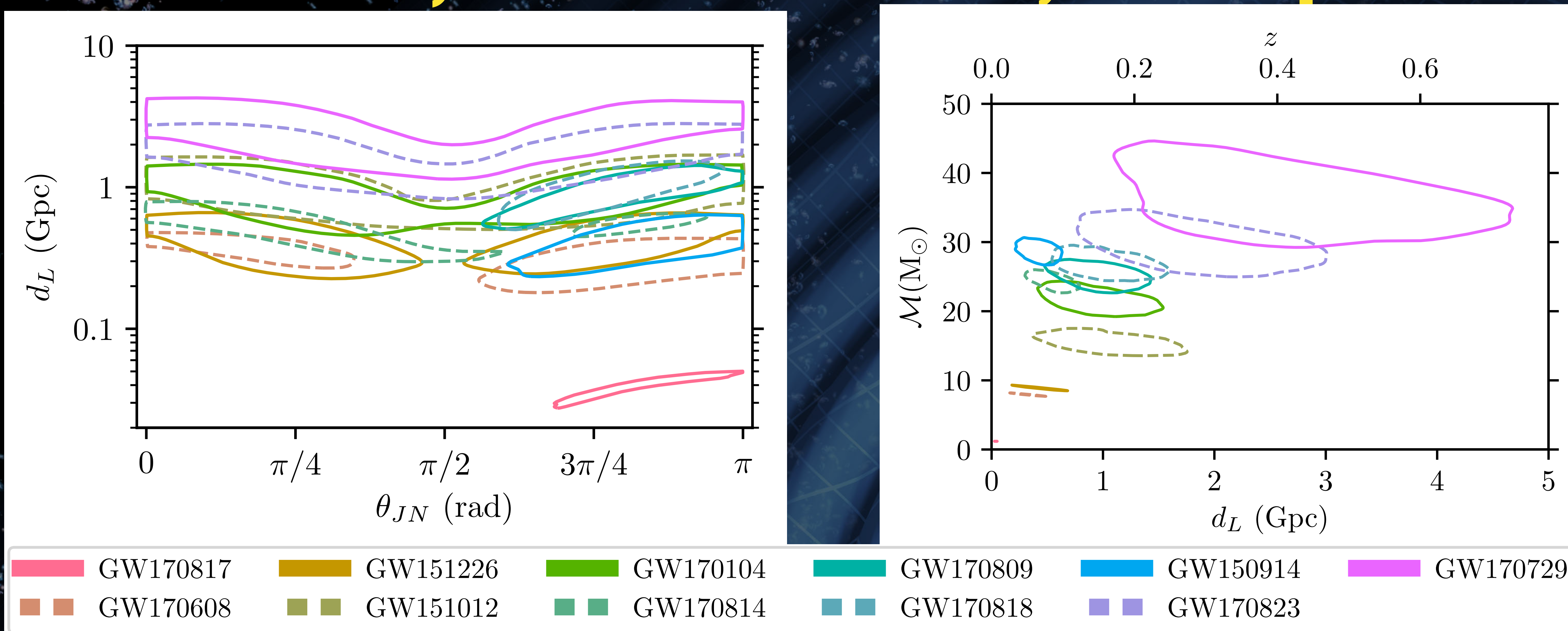

- GW170817: most distant BBH, d_L=2750 (+1350,-1350) Mpc
- GW170608: closest BBH, d_L=320 (+120,-110) Mpc
- GW170817: BNS, d_L=40 (+10,-10) Mpc
- Degeneracy between the distance and the binary's inclination
- Inclination angle has a bimodal distribution around θ_{JN}=90°
- Luminosity distance and chirp mass are positively correlated

Sky location

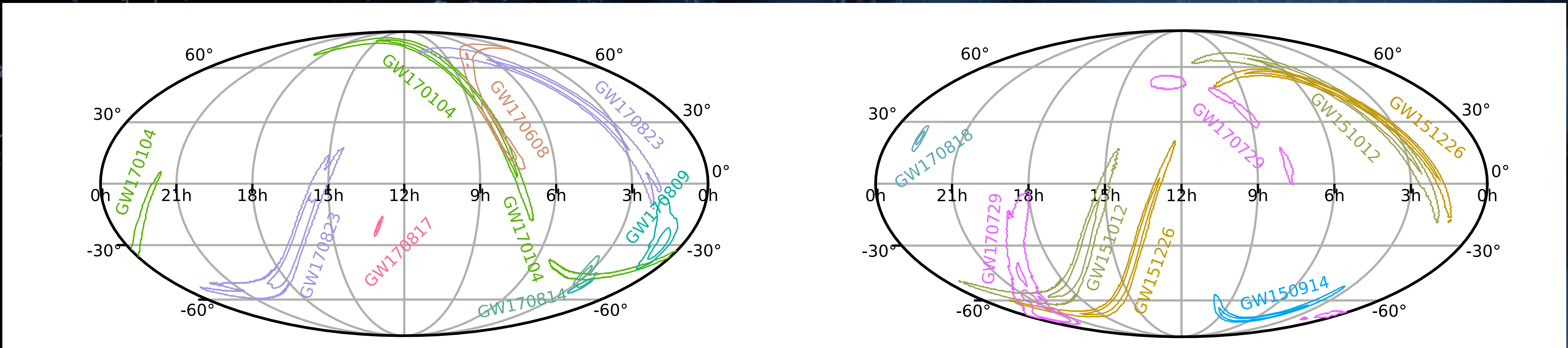

O2 GW events for which alerts were sent to EM observers.	O1 + GW170729, GW170818 (not previously released to EM observers)

- **Inclusion of Virgo improves sky localization:** importance of a global GW detector network for accurate localization of GW sources
- **GW170818** (LV) is <u>best localized BBH</u> to date: with a 90% area of <u>39 deg^2</u>
- GW170729 was not identified by the low-latency searches
- Virgo trigger was not included in the significance estimation of GW170818, so as L-only trigger it did not pass the false alarm threshold of the online searches

GW170817 update

high-spin prior $a_i < 0.89$

low-spin prior $a_i < 0.05$

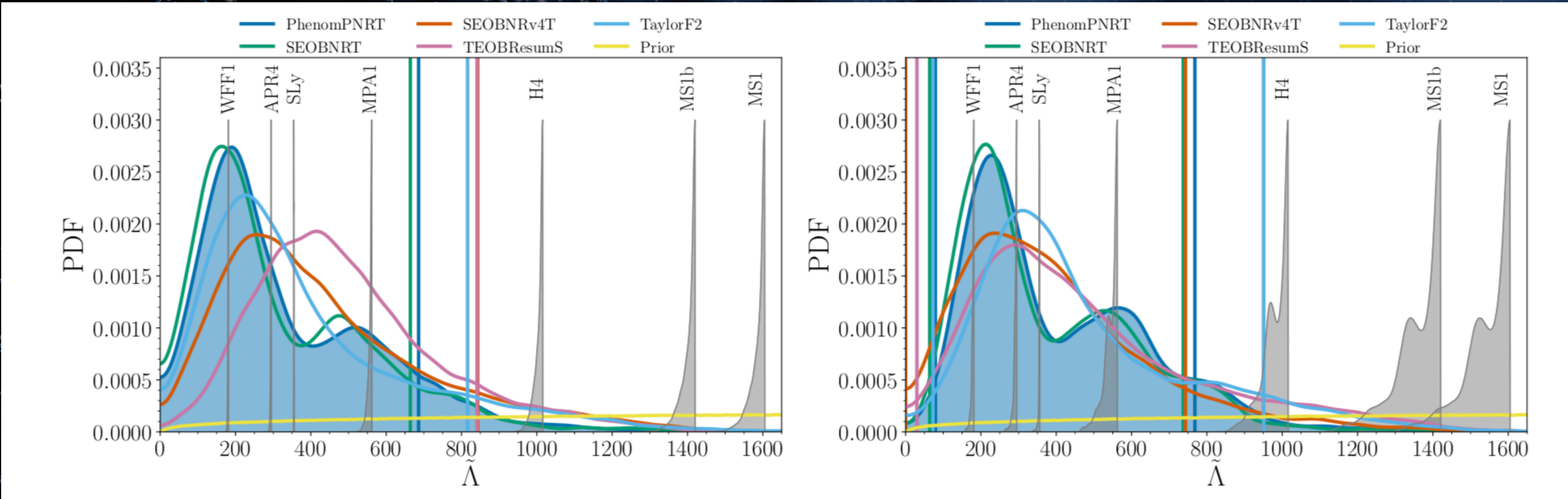

- **All O2 events reanalysed with recalibrated data**
  - Results are consistent with previously published ones
  - Bounds on the effective tidal deformability are about 10% wider than reported previously

BBH & BNS rates estimates

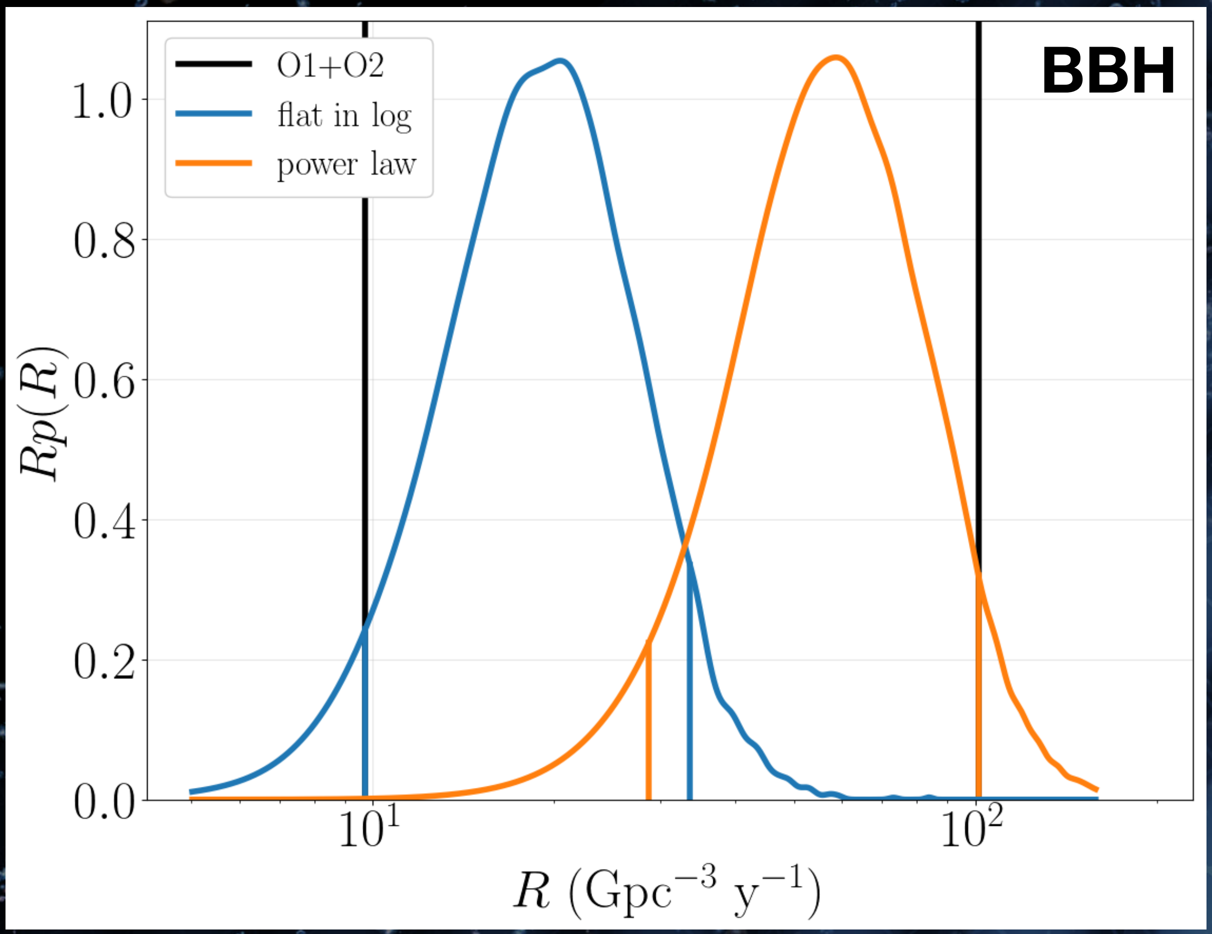

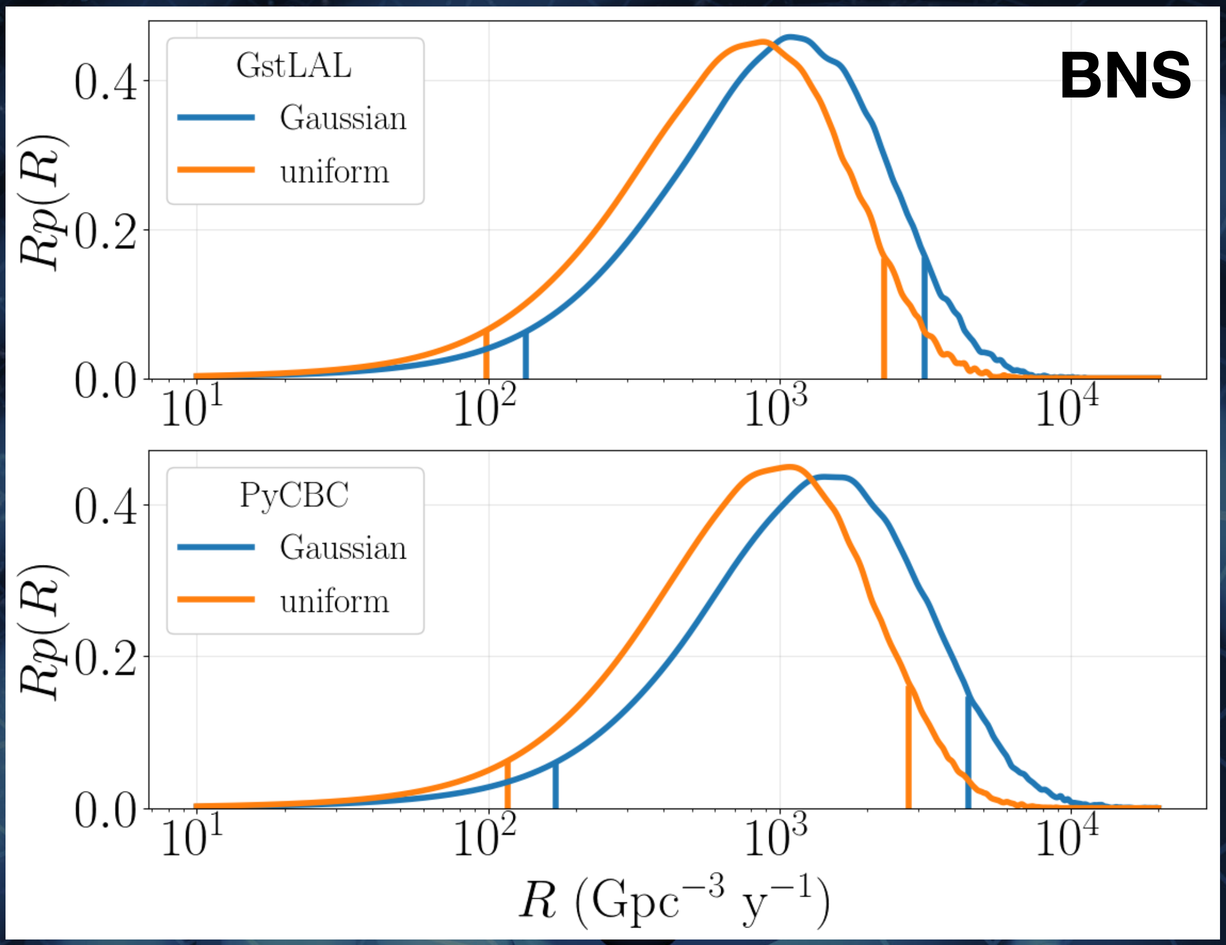

- BBH: Two distribution of primary mass:
  - Uniform in log
  - Power law $p(m_1) \propto m_1^{-\alpha}$ with α=2.3
- [5,50] $M_\odot$
- Union of intervals: **9.7-101 Gpc^{-3} y^{-1}**

- BNS: Two populations:
  - Uniform component masses in 1-2 $M_\odot$ range
  - Two uncorrelated gaussians (overall mass distribution centered at 1.33 $M_\odot$ with standard deviation 0.09 $M_\odot$)
- Compatible with previous results
- **110-3840 Gpc^{-3} y^{-1}**

NSBH Event Rates

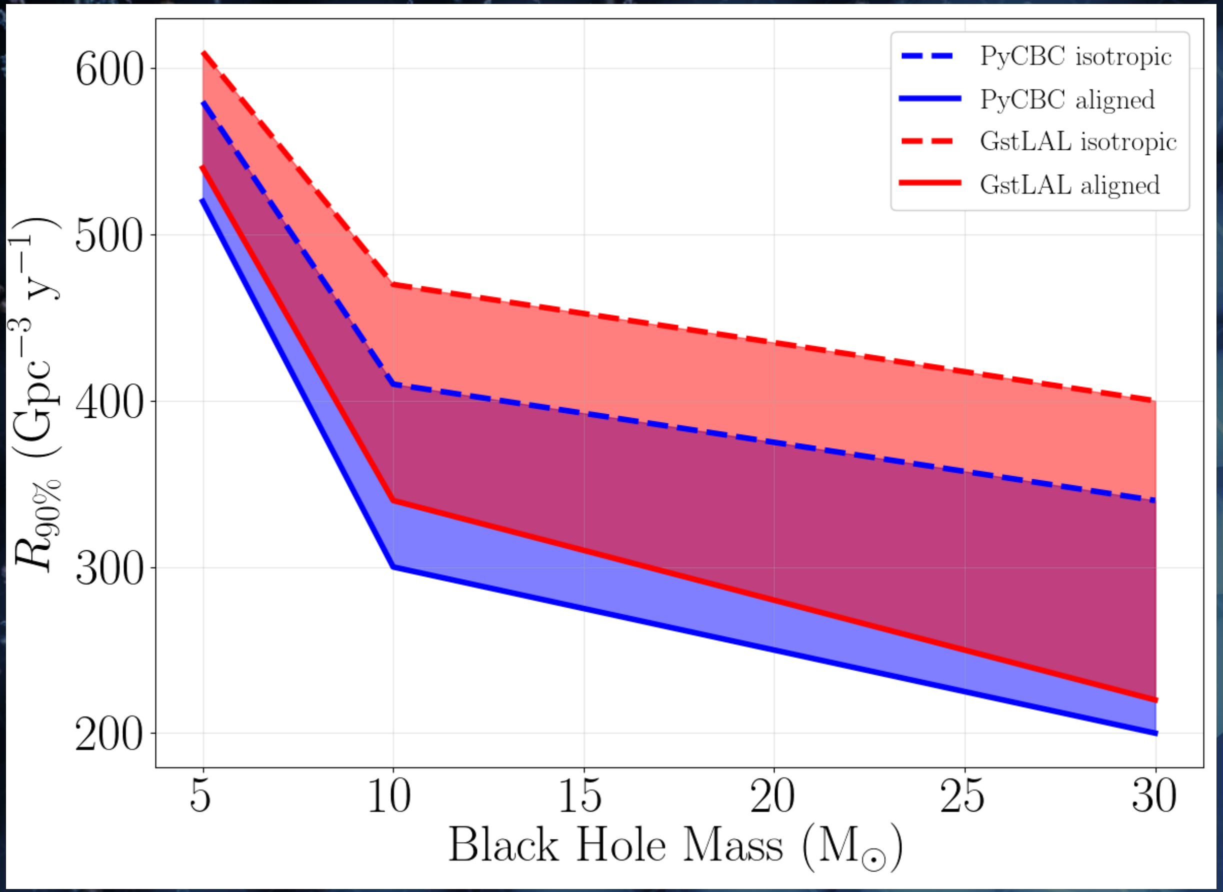

Neutron Star Black Hole (NSBH)

- Difficult space to model
- Assume 2 spin configurations: aligned-spin, isotropic
- All upper limits are below **610 Gpc^{-3} y^{-1}**

O1-O2 merger population study

Binary Black Hole Population Properties Inferred from the First and Second Observing Runs of Advanced LIGO and Advanced Virgo

`dcc.ligo.org/LIGO-G1802242 (arXiv:1811.12940)`

Based on the observed sample of 10 BBH, Bayesian inference on mass, spin and redshift models:

- ⋆ GW merger rate distribution relation to mass and mass ratio functions,
- ⋆ Spin amplitude and orientation distribution,
- ⋆ Merger rate vs redshift.

O1-O2 sources and their progenitors

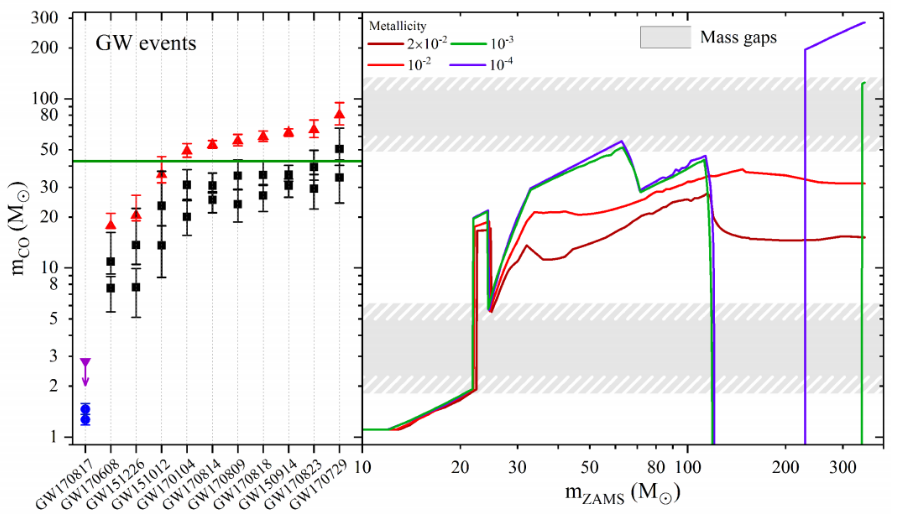

ZAMS models at various metalicities by Spera & Mapelli (2017)

Mass distribution for O1 events + GW170104

- Simple one-parameter model – power law index
- Flat in m_2 from m_{min} to m_1
- $m_{min} = 5$, $m_{max} = 100\ M_\odot$

$$p\left(m_1, m_2\right) \propto m_1^{-\alpha} \frac{1}{m_1 - m_{\rm min}}$$

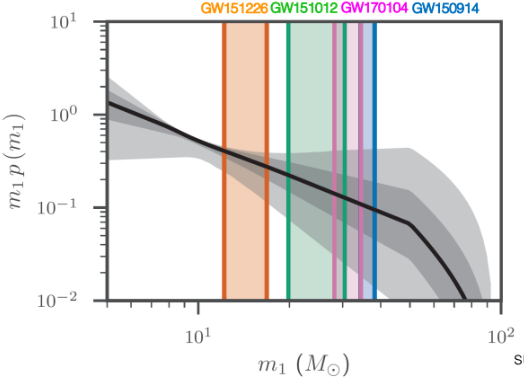

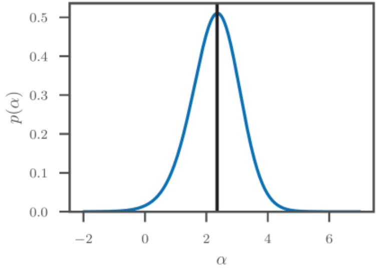

LVC, Phys. Rev. Lett. 118, 221101 (2017)
supplement: https://dcc.ligo.org/LIGO-P170104/public

O1-O2 mass distribution models

$$p(m_1, m_2 | m_{\min}, m_{\max}, \alpha, \beta_q) \propto \begin{cases} C(m_1) m_1^{-\alpha} q^{\beta_q} & \text{if } m_{\min} \le m_2 \le m_1 \le m_{\max} \\ 0 & \text{otherwise} \end{cases}$$

Models A,B

Fishbach & Holz (2017), Wysocki (2018), Kovetz et at (2017), Talbot & Thrane (2018)

Model C

Talbot & Thrane (2018)

includes Gaussian to capture build-up of high-mass BHs from pulsational pair instability (PPSNe), from stars with initial mass $100 \le M_{init} \le 150\ M_\odot$

- λ_m : mixture parameter
- $\mu_m\ \sigma_m$: Gaussian parameters
- δm: low mass tapered turn on

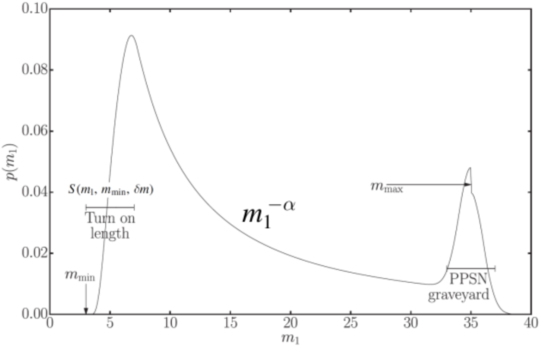

$$p(m_1|\theta) = \left[(1-\lambda_m) A(\theta) m_1^{-\alpha} \Theta(m_{\max} - m_1) + \lambda_m B(\theta) \exp\left(-\frac{(m_1 - \mu_m)^2}{2\sigma_m^2} \right) \right] S(m_1, m_{\min}, \delta m),$$

$$p(q|m_1, \theta) = C(m_1, \theta) q^{\beta_q} S(m_2, m_{\min}, \delta m).$$

Merger rates with mass, mass ratios dependence

- Merger rate with mass dependence
  - Model A/B: Light more frequent than heavier
  - Model C: **lnBF ~ 2** for build up (Gaussian) at high masses
- Mass ratios
  - near flat or declining
  - most asymmetric mergers disfavored

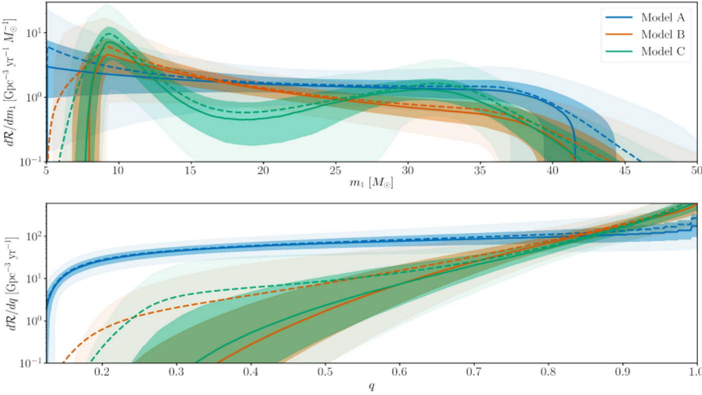

99th percentile of the mass distribution (M_{max} cut-off):

- ⋆ Model A: $43.8 M_\odot$
- ⋆ Model B: $42.8 M_\odot$
- ⋆ Model C: $41.8 M_\odot$

⋆ $\alpha(A) = [-1.5, 1.7]$

$\alpha(B) = [-0.1, 2.9]$

⋆ $R_0(A) = [30, 140]\ Gpc^{-3}\ yr^{-1}$

$R_0(B) = [25, 110]\ Gpc^{-3}\ yr^{-1}$

Spin amplitude distribution results

- Parametric distribution, marginalizing over all mass and spin tilt / mixture parameters
  - Some preference for spins which decline away from zero
- Non-parametric 5 bin analysis, fix tilts to isotropic or *exactly* aligned
  - Aligned distribution favors lower spins
  - Isotropic spins mostly flat

$$p(a_i|\alpha_a, \beta_a) = \frac{a_i^{\alpha_a - 1}(1 - a_i)^{\beta_a - 1}}{\mathrm{B}(\alpha_a, \beta_a)}$$

$$p(\cos t_1, \cos t_2|\sigma_1, \sigma_2, \zeta) = \frac{(1-\zeta)}{4} + \frac{2\zeta}{\pi} \prod_{i \in \{1,2\}} \frac{\exp\left(-(1-\cos t_i)^2/(2\sigma_i^2)\right)}{\sigma_i \mathrm{erf}(\sqrt{2}/\sigma_i)}.$$

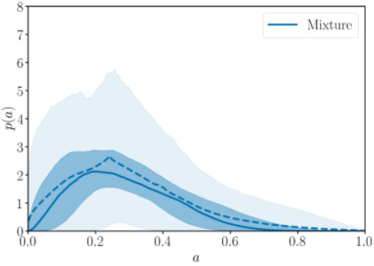

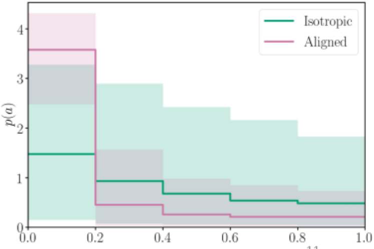

Evolution of the merger rate with redshift z

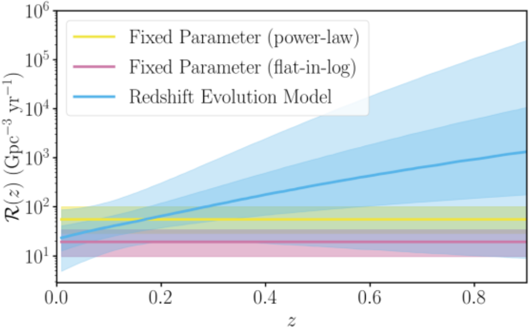

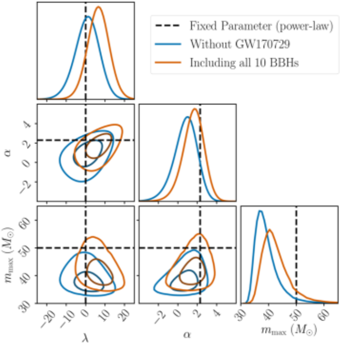

$$\frac{dR}{dm_1 dm_2}(z) = R_0 p(m_1, m_2 \mid \alpha, m_{\max})(1+z)^\lambda$$

- Significant correlation between λ and α
- *Prob*$(\lambda \geq 0.) = 88\%$
- Result depends on whether GW170729 (at z~0.5) is included.
- Expect significant improvement as more BBH mergers are accumulated.

Conclusions (rates and populations)

- ⋆ Low-mass binaries more frequent than high mass,
- ⋆ Difficult to probe the lower mass gap (not enough volume-time sensitivity below $5\,M_\odot$),
- ⋆ Heavy BH constraints: most BH $< 45\,M_\odot$,
- ⋆ Hint of a second (massive) population component,
- ⋆ Spin distribution disfavors extremely high spins under aligned scenario,
  - ⋆ isotropic spins less constrained.
- ⋆ Rate evolution with redshift: increasing with redshift and uniform in comoving volume are favored.

Conclusions (catalog)

- In O1&O2 LIGO and Virgo have confidently detected GWs from 10 BBH and one BNS,
  - One GW event every 15 days,
- Merger rates (based on fixed population):
  - BBH: 9.7 - 101 $\mathrm{Gpc}^{-3}\ \mathrm{y}^{-1}$
  - BNS: 110 - 3840 $\mathrm{Gpc}^{-3}\ \mathrm{y}^{-1}$
  - NSBH 90% upper limit: 610 $\mathrm{Gpc}^{-3}\ \mathrm{y}^{-1}$
- No component masses observed in the mass gaps ($< 5\,M_\odot$ and $50 - 150\,M_\odot$),
- No significant detection of precession or higher-order modes.

Data available from the GW Open Science Center:
`www.gw-openscience.org/catalog`

Towards O3

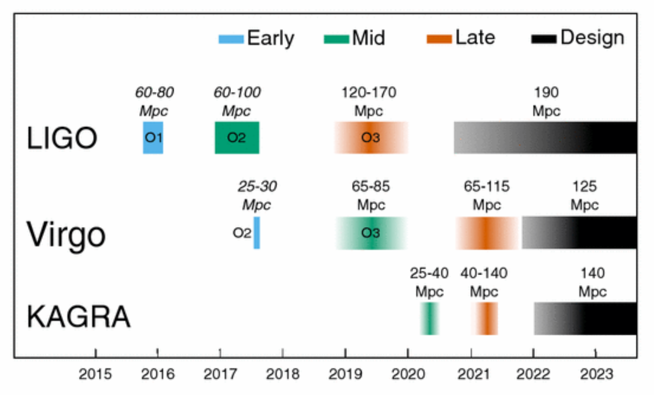

⋆ Open public alerts in O3 (GCN circulars), see `emfollow.docs.ligo.org/userguide` for documentation.

⋆ In addition to tens of BBHs, we expect 1-10 BNS events, with median localization accuracy in terms of 90% credible area of 120–180 deg^2 (10–20% localized to less than 20 deg^2).

+

Lensed GW events in the GWTC-1?

Event	$m_1/M_\odot$	$m_2/M_\odot$	$\mathcal{M}/M_\odot$	$\chi_{\rm eff}$	$M_{\rm f}/M_\odot$	$a_{\rm f}$	$E_{\rm rad}/(M_\odot c^2)$	$\ell_{\rm peak}/({\rm erg\,s^{-1}})$	$d_L/{\rm Mpc}$	z	$\Delta\Omega/{\rm deg}^2$
GW170809	$35.2^{+8.3}_{-6.0}$	$23.8^{+5.2}_{-5.1}$	$25.0^{+2.1}_{-1.6}$	$0.07^{+0.16}_{-0.16}$	$56.4^{+5.2}_{-3.7}$	$0.70^{+0.08}_{-0.09}$	$2.7^{+0.6}_{-0.6}$	$3.5^{+0.6}_{-0.9} \times 10^{56}$	990^{+320}_{-380}	$0.20^{+0.05}_{-0.07}$	340
GW170814	$30.7^{+5.7}_{-3.0}$	$25.3^{+2.9}_{-4.1}$	$24.2^{+1.4}_{-1.1}$	$0.07^{+0.12}_{-0.11}$	$53.4^{+3.2}_{-2.4}$	$0.72^{+0.07}_{-0.05}$	$2.7^{+0.4}_{-0.3}$	$3.7^{+0.4}_{-0.5} \times 10^{56}$	580^{+160}_{-210}	$0.12^{+0.03}_{-0.04}$	87

- ⋆ `arXiv:1901.03190` - similarity in amplitude phase and sky position of GW170809 and GW1070814.

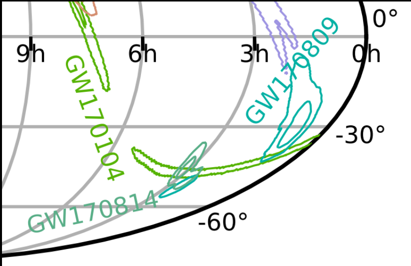

- ⋆ `arXiv:1901.02674` - compare the full posteriors, compute the ratio of the Bayesian evidences of the lensed and unlensed hypotheses: